

MILLIKEN CLEAN COAL TECHNOLOGY DEMONSTRATION PROJECT

COMPARISON OF *ESPerf*[™] MODEL PREDICTIONS WITH UNIT 2 ELECTROSTATIC PRECIPITATOR PERFORMANCE

INTERIM REPORT

Prepared by:

CONSOL Inc.
Research & Development
4000 Brownsville Road
Library, Pennsylvania
15129-9566

New York State Electric & Gas
Corporation
Corporate Drive
Kirkwood Industrial Park
P.O. Box 5224
Binghamton, New York
13902-5224

Principal Investigator
J. T. Maskew

Principal Investigator
B. Marker

Prepared for:

U. S. Department of Energy
Milliken Clean Coal Technology
Demonstration Project
DE-FC22-93PC92642

New York State Electric & Gas
Corporation
Corporate Drive
Kirkwood Industrial Park
P.O. Box 5224
Binghamton, New York
13902-5224

Electric Power Research Institute
3412 Hillview Avenue
P. O. Box 10412
Palo Alto, California
94303

Empire State Electric Energy
Research Corporation
1515 Broadway, 43rd Floor
New York, New York
10036-5701

New York State Energy Research
and Development Authority
Two Rockefeller Plaza
Albany, New York 12223

November 1997

ABSTRACT

The performance of an electrostatic precipitator (ESP) model (*ESPerTM*) was evaluated for a 160 MW_e pulverized coal-fired power plant firing a medium sulfur, bituminous coal. The ESP was recently modified to improve its effectiveness. New internals, computer controlled transformer-rectifier sets and a third field were installed. The plates have a 16-inch plate spacing. The *ESPer* model, developed for EPRI, consistently under predicted the effectiveness of the ESP at full load.

SUMMARY

The *ESPert*TM ESP model was evaluated by comparing the predicted performance with actual ESP performance measured at Milliken Station Unit 2 of the New York State Electric & Gas Corporation (NYSEG). Milliken Station is an electric utility station with two 160 MW_e pulverized coal-fired steam generators. As part of the modifications required for installation of a flue gas desulfurization system, the Unit 2 ESP was modified. New internals were installed with a wide, 16-inch plate spacing. Computer controlled transformer-rectifier (TR) sets were added. This evaluation shows that the ESP model significantly under predicts the performance of the Milliken ESP when firing a medium sulfur bituminous coal. Corrections to the *ESPert* model improved the prediction but could not fully resolve the differences. The model appears unable to predict the effect of the wide plate spacing adequately. Diagnostic messages confirm that the operating conditions for this ESP are outside the range expected by *ESPert*. Additional tests with other coals should be undertaken to define the effects of wide plate spacing.

DISCUSSION

Background

NYSEG's Milliken Station was extensively modified to accommodate a wet scrubber, flue gas desulfurization system. Modifications included upgrading the ESPs on both units. Originally, Unit 2's particulate control consisted of two ESPs in series, stacked one on top of the other. The bottom unit was removed completely while the top unit was rebuilt and an additional, third field added. The internals of the top ESP were replaced using a wide plate spacing design by Belco Technologies Corp. New, computer controlled TR sets were also installed. The physical characteristics of the old and new ESPs are shown in the following table.

Precipitator Characteristics

	Original ESP ¹		New ESP
	Lower ESP	Upper ESP	
Date Built	1955-58	1971-74	1993
Plate Spacing, inches	8 ¾	9	16
Plate Height, feet	20	30	30
Fields	2	2	3
Field Depth, feet, each	9	9	9
Gas Velocity, fps	5.7	3.4	3.7
SCA, ft ² /1,000 acfm gas @ full load	150	242	175

As shown in this table, the plate spacing was increased from approximately nine inches to sixteen inches while the total number of fields decreased from four to three. The SCA at full load decreased from 392 to 175 ft² per 1,000 acfm of flue gas. The efficiency of the original ESP was 99.43% on a 1.54 wt % sulfur coal. For a 3.2 wt % sulfur coal, the efficiency was 99.65%. After the retrofit, the efficiency increased to 99.9% for a 1.75% sulfur coal.

Currently the Milliken Unit 2 ESP consists of two separate, parallel sections: a south, or "A", ESP and a north, or "B", ESP. Gas flow is evenly split between these sections dividing upstream of the air heater and rejoining at the scrubber. Each side has an additional divider wall that runs the length of the ESP box. The south and north sides are identical, parallel precipitators with separate TR sets enclosed in a single box.

In October 1995, the performance of the Unit 2 ESP was evaluated while firing a medium sulfur (1.75 wt % sulfur), bituminous coal in the boiler. Field tests were conducted to collect inlet and outlet particulate concentrations and flue gas data for each side of the ESP separately. The results of these tests are compared with the

performance predictions made by *ESPert™*, an ESP model developed by Peter Gelfand of P. Gelfand Associates under the auspices of EPRI. The *ESPert* computer model was produced from algorithms developed by the Southern Research Institute. Version 4.2 was used, in the DOS operating system on a PC compatible, Intel 486 PC.

For comparison of the results, the two sides of the ESP were treated as separate, independent units each treating one-half of the flue gas exiting Unit 2. The design parameters of Unit 2 were adjusted accordingly for *ESPert*. Some design parameters were adjusted as requested by Peter Gelfand. These changes will be discussed later.

Data Sources

Data required by the *ESPert* model were obtained from three sources: the field test report² of the ESP performance; the Milliken Station data logger; and data provided by NYSEG personnel. The first source, the field report, details the testing procedure for the Milliken Unit 2 ESP and the results of the performance tests. This report provided the flue gas conditions and particulate statistics as measured at the inlet and exit of both the north and south sides of the Unit 2 ESP. Appendix A lists the coal and ash analyses and the particulate size data excerpted from this field report. Gas flow rates, humidity and temperatures measured during the field test is included in Appendix B. The Milliken data logger provided general operating conditions and an indication of boiler and ESP operating stability during the field test. Averages of the operating parameters required by *ESPert* are listed in Appendix B; selected instantaneous values will be presented later. NYSEG personnel provided station and ESP design specifications, and air load voltage-current (V-I) data for the V-I curves required for the ESP performance calculation. This information is tabulated in the Appendices C and D, respectively.

The ESP field report discusses the test methods and results of duplicate testing of the Unit 2 ESP. The north and south sides were tested separately and are individually compared with their respective *ESPert* predictions. Inlet and exit data were obtained from the field report for several parameters. The following parameters are included in this report:

- Total particulate matter (PM)
- Particle size distribution
- Flue gas composition (O₂ and H₂O)
- Volumetric flue gas flow rate
- Flue gas temperature
- Actual fly ash resistivity at the Inlet

For additional measurements, refer to the original field performance report.

Coal and ash samples were collected during the field test and analyzed. Analyses of the daily composites of the coal samples were consistent within analytical error and their average was used for the *ESPert* calculations. The fly ash analyses also were

averaged.

Two days of sampling were employed for each side of the ESP. While the repeat trials for each side of the ESP were consistent, the result of each individual test was compared with a model prediction rather than using an overall average of the runs on the north and south sides. The required run data are listed in Appendix B.

Four sets of inlet and outlet particle size data were collected during the field test, two sets for each side of the Unit 2 ESP. The calculated D_{50} and cumulative weight percents are tabulated in the Appendix A. These results were plotted on Rosin-Rammler coordinates to obtain an estimate of the performance for the minus 10 μm and minus 2.5 μm fractions. The minus 10 μm and minus 2.5 μm fractions were estimated directly from the data with no smoothing or curve fitting.

During this field test program, five trials collecting gas flow, temperature and total particulate data were conducted on the north-side ESP and three on the south. Of these, North #1, #3 and #4 and all three south trials sampled the inlet and outlet streams simultaneously. These six trials are compared with ESP performance predicted by the model. Total particulate concentrations into and out of one side of the ESP were collected as part of the procedure for each trial. This was used to calculate the penetration. Penetration is:

Penetration = 100 & Percent Removal

or

$$\text{Penetration} = 100 \times \left[\frac{\text{Concentration of Solids in Outlet}}{\text{Concentration of Solids in Inlet}} \right] \cdot 100$$

Penetrations for the minus 10 μm and minus 2.5 μm fractions were calculated using the daily particle size data. The size test provided the size distribution for the total particulate concentrations conducted on the same day. Thus,

$$\text{Penetration, } < 10 \mu\text{m Frac.} = 100 \times \left[\frac{(\text{Outlet Size, } < 10 \mu\text{m Frac.}) \cdot (\text{Conc. of Solids in Outlet})}{(\text{Inlet Size, } < 10 \mu\text{m Frac.}) \cdot (\text{Conc. of Solids in Inlet})} \right]$$

The equation for the minus 2.5 fraction is similar.

ESPer used the sample D_{50} and the log-normal standard deviation of the distribution calculated from the inlet particle size data to generate a size distribution for its calculation procedures. P. Gelfand Associates recommended having the program generate 21 size fractions rather than using actual data. This was recommended because of the way *ESPer* treats this data internally. Gelfand recommended values

for several other parameters. These are indicated in the appendices by enclosing the value in square brackets, [].

For the actual ash resistivity, an average of the results of the four days of testing was used (4.31×10^{10} ohm-cm). As shown in Figure 1, the actual ash resistivities (AR) are consistent. These resistivities lie between the curves predicted from the two resistivity algorithms in *ESPert*. The algorithms that include SO₃ effects are referred to as Model 1 and Model 2. The measured resistivities agree closely with the values predicted by Model 1, showing a similar, slight increase with increasing temperature. Model 2 resistivities are much lower. No bias was evident in the horizontal position of the sample port used for obtaining the resistivity value, as shown in Figure 2. The measured resistivities are listed in Appendix A. It should be noted that *ESPert* recommends using the Model 2 resistivity algorithm for predicting ESP performance in the event actual resistivity measurements are unavailable.

Figures 3-6 show selected operating parameters for October 17-20, 1995. After reaching maximum generation capacity, approximately 157 MW_e, gross, operation of the Unit 2 boiler/generator was stable. Each afternoon, the flue gas temperatures at the inlets to the north and south sides of the ESP increased slightly. This was probably due to the increasing ambient air temperatures. This would reduce the flue gas cooling provided by the combustion air in the heat pipe air heaters upstream of the ESP.

Figures 7-18 show the electrical readings from the TR sets. Figures 7-9 show the primary voltage and current, and the secondary voltage and current for TR Sets 2-B1, 2-B2 and 2-B3, the north-side ESP TR sets, on October 17, 1995. Similarly, Figures 10-12 show these readings on October 18, 1995. Figures 13-15 show the V-I readings for TR Sets 2-A1, 2-A2 and 2-A3, the south-side ESP TR sets, on October 19, 1995, while Figures 16-18 are for October 20, 1995. These periods correspond to the trials on each side of the Unit 2 ESP. The figures show that after the generation lined out at the maximum on October 17, the operation of the TR sets was steady.

Figures 19-22 are Rosin-Rammler plots of the inlet and exit particle size data from the samples collected simultaneously in four trials on October 17, 18, 19 and 20, respectively. The samples from October 17 and 18 were collected on the north-side of the ESP, while the remaining two are from the south-side. This corresponds with the inlet/outlet flue gas sampling on each side of the Unit 2 ESP. The results show low variability for the plus one μm material, as shown in Figures 23 and 24. Good agreement was obtained for the duplicate tests on each side of the ESP and between the two sides. Only the inlet D₅₀ and log-normal standard deviation are used by *ESPert*.

Besides the fuel and particulate data discussed above, *ESPert* requires boiler and TR set operating conditions for each run evaluated. This is tabulated in Appendix B. Note that some values requested are for the entire site. Since each side of the ESP was treated separately, some values were adjusted to reflect this. The adjusted values are shown enclosed in parentheses, (). The data enclosed in square brackets, [], were

recommended by P. Gelfand. Data followed by an asterisk, *, were measured at the inlet or outlet to the ESP during the performance field trial.

Design specifications for the ESPs built by Belco Technologies Corp. are tabulated in Appendix B. The order of the specifications is similar to that required by the *ESPert* model. The model also requests general information about the generation facility. This is contained as well in Appendix B.

ESPert requires operating or full load V-I data to predict operating behavior. Air load V-I data were used since full load data could not be obtained without requesting a variance. These values, listed in Appendix D, were entered into *ESPert* as full load data according to Gelfand's recommendation. The various V-I correlations generated by *ESPert* are plotted along with the actual data on Figures 25-30. The model requires non-zero data and has only a limited number of inputs; thus, only the odd (or even) numbered, non-zero points were used. Correlations generated by the model appear to agree with the data. Included on these figures are the correlations estimated by *ESPert*. Each correlation is found immediately below its associated plot.

***ESPert* Comparison**

The test results presented above were compared with the removals of fly ash predicted by *ESPert*. Operational data, listed in Appendix B, along with design specifications (Appendix C) were entered into *ESPert* according to the procedures discussed in the user's manual³. The air load V-I values listed in Appendix D were substituted for full load data. Otherwise, the normal procedure was followed. Both algorithms used to predict ash resistivity in the ESP model and the AR were explored in this evaluation.

ESPert consistently predicted lower efficiencies than measured at the Milliken ESP. Overall, predicted penetrations using the Model 2 resistivity agreed with those predicted using the AR but were much higher than measured penetrations. Using the Model 1 resistivity, the predicted penetrations were two to three times higher than those predicted by the other resistivities. While Model 1 closely predicts the observed resistivity, it does not predict the ESP efficiencies as well as Model 2. For the finer fractions, the predicted penetrations are closer to the observed values. The reasons for this trend are not known.

Figures 31, 32 and 33 illustrate the measured and predicted penetrations at Milliken Station Unit 2. Shown are the measured penetrations along with those predicted by *ESPert* using the AR and the Model 1 and Model 2 ash resistivities. The penetrations for the minus 10 μm and minus 2.5 μm fractions are based on that fraction of the inlet particulate. The average measured penetration for the six tests is also included in these figures as a thick horizontal line. Figure 31 is for the total ash. The minus 10 μm fraction is plotted in Figure 32. Similarly, the minus 2.5 μm fraction is plotted in Figure 33. In addition to the total penetration, the penetrations of these two size fractions are predicted by *ESPert*.

As shown in Figure 31, the measured total penetration is consistently lower than the prediction. Penetrations predicted using the AR and Model 2 resistivity agree with each other and are closer to the measured value than those using the Model 1 resistivity. Compared with the average penetration observed for these six runs, the AR and Model 2 predictions are six to seven times higher than the measured penetrations with Run S3 having the largest error. Run S3 has a higher gas rate, suggesting that this may be one reason that this penetration is underestimated to a greater degree. However, this does not explain the general lack of agreement. The Model 1 predictions are two to four times higher than the AR or Model 2 predicted penetrations; this was unexpected since the Model 1 resistivity is closer to the measured resistivity (or AR).

Similarly, for the minus 10 μm fraction, Figure 32, the Model 1 penetration prediction is the least accurate. The AR and Model 2 penetrations are 4.5 to 6 times the average measured value, while the Model 1 predictions are again 2 to 4 times higher than the other predictions. Thus, the Model 1 predictions are 10 to 22 times higher than the average measured penetration. The penetration predictions are highest for Run S3 as was the case for the total penetration.

The predicted penetrations of the minus 2.5 μm fraction are shown in Figure 33. For the AR and Model 2 resistivity, these penetrations are within the experimental error from the average measured value. However, they are consistently higher than the measured penetrations varying between 1.2 and 2 times higher, suggesting some potential bias. Again the Model 1 value is much higher, 3 to 5 times the measured penetrations. While the amount of material in this fraction is very small, it appears that the *ESPert* model adequately predicts this fraction.

Adjustments to *ESPert*

Two of the possible reasons for this high estimate of penetration are the design basis of *ESPert* and the difference between operating and air load V-I curves. The *ESPert* model was developed using data from ESPs with a closer, predominately 9-inch plate spacing. This may explain in part the reason for its overestimation of penetration. A second possibility is that the operating V-I curves are significantly different from the air curves used in these predictions. While checking the first hypothesis is not possible, the second one will be examined next.

Replotting the V-I curves presented in Figures 25-30 and including the V-I data collected during the runs produces Figures 34-39. The lead TR set on each side of the ESP displays a significant shift in the ESP voltage for a given primary voltage as shown on Figures 34 and 37. The ESP current also decreases for a given ESP voltage. For the other four TR sets, the differences between the air load curve and operating data points are small. The thin, solid lines in these figures represent revised correlations that pass through the operating point but have the same slope (or power) as the original correlation. The revised correlations are listed below their respective plots. These new correlation coefficients were inserted into the *ESPert* model and two of the

runs, Run N1 and S3, reevaluated.

Sneakage and the velocity sigma are two other *ESPert* variables that affect the agreement between the measured penetrations and predicted values. These variables affect all particle sizes. These were changed in combination with the V-I adjustment. Default values for sneakage and the velocity sigma are 0.05 and 0.15. The default values were reduced to 0.03 and 0.07, respectively. These adjustments represent a considerable improvement in the amount of sneakage and the velocity/temperature distribution across the ESP inlet.

These adjustments were applied to Runs N1 and S3, and the predicted penetrations plotted in Figures 40 and 41, respectively. The predictions are compared with the average penetration result from the six runs. The average measured penetration, original prediction, and four adjusted predictions -- V-I adjustment alone and combined with adjustments for sneakage, velocity and both sneakage and velocity -- are plotted for the total particulate, the minus 10 μm fraction and the minus 2.5 μm fraction. The bars are labeled to indicate the ratio of the predicted penetration to the average measured penetration.

Adjusting for the V-I correction accounts for about 40% of the higher penetration of the total particulate and the minus 10 μm fraction. The sneakage and velocity sigma adjustments reduce it an additional 10% compared with the original prediction. Applying these corrections to the minus 2.5 μm fraction, the predicted values closely approximate the average measured penetrations. For Run N1, the predicted minus 2.5 μm values are less than the measured values.

The apparent trend to predict higher removals for the smaller particles could be an artifact of the methodology used internally to create the size distribution. A log-normal curve is used to approximate the ESP inlet size data. As shown in Figure 41, the size data are not linear on a log-normal plot below 2.5 μm . Most of the minus 2.5 μm fraction appears to be very small, causing *ESPert* to over estimate the removal of this fraction. Thus, the apparent agreement with this fraction may be just a coincidence.

It appears that *ESPert* under predicts the improvement of the 16-inch plate spacing and predicts higher removals of the finest material than was observed. These predictions were developed using the AR for the resistivity value, but the Model 2 resistivity predictions were similar.

Overall, the *ESPert* model under predicts the removals of the larger fractions at Milliken Station resulting in higher predicted penetrations than observed at Milliken. These differences are greater than the error limits of the original data Southern Research Institute used for developing the algorithms⁴. For small size fractions, the predictions are also over estimated, but are within the accuracy of the original data.

Diagnostic Reports

*ESPer*t provides the option of diagnosing the performance of individual TR sets. Diagnostic reports were created for all six runs discussed above for the AR, Model 1 and Model 2 resistivities. The same messages were often repeated, which is expected since the data sets are very similar. They often repeated depending upon the position of the individual TR set. Some difference was noted between resistivity models.

For TR Set 1, “Low ESP Current; Increased Resistivity” was produced for every Model 2 run, while the AR and Model 1 resistivities were “In Predicted Range”. The Model 2 runs also included other messages as listed below:

- Failure of Automatic Voltage Control, False Detection of Sparcs/Arcs
- Reduced Clearances
- Dust Build-Up on Collecting Electrode
- High Levels of Carbon in Fly-Ash
- Air In-Leakage into ESP Casing
- Air In-Leakage into Hopper, and
- Boiler Tube Leaks.

For the second TR set, all of the north runs and the Model 2 south runs were “In Predicted Range”, but the AR and Model 1 runs had predicted current problems. The diagnostic messages for these cases on the south-side of the ESP said “High ESP Current Detected” and “Sparking Rate High, Return AVC”,

TR Set 3 had only one report: “Defective Limit Circuit / SCR Shorted”. This was displayed for every run and for each resistivity.

The ESP appeared to be operating normally with no indication of any problems. The on-site Belco representative also stated that the operation was normal. No indication of problems with any of the units was observed and the spark rate was low. Thus, the diagnostics generated by the model did not match the operating experience. Again this may be a result of trying to extend the results from ESPs with a narrower plate spacing to the 16-inch spacing present in the Milliken ESP.

Limitations of *ESPer*t

Users of this model should note two limitations. First, data cannot be saved directly under a new filename in *ESPer*t. Instead, copies are made in DOS (or Windows) and edited in *ESPer*t to include the data for new trials or units. Secondly, the last TR set will zero out whenever a performance prediction is run with the actual V-I data included for this TR set. That is, the V-I data will disappear and the correlation coefficients will be reset to zero if V-I data are present for the final TR set. The coefficients must be manually entered for the last TR set. As discussed above, the model also repeated the diagnosis notes for all of the evaluated TR sets. This may be a limitation due to the improved control system of the Belco units or the wide plate spacing in these units.

Conclusions

Predictions of ESP penetration using the *ESPert* model are high for an ESP with 16-inch plate spacing firing a medium sulfur bituminous coal. The resistivity estimates for the Model 1 method are close to the actual measurements, but provide much worse estimates of ESP effectiveness than does Model 2's resistivity. Model 2's estimate for resistivity is much lower than the measured value, but the effectiveness estimates are identical.

The Milliken Unit 2 ESP has wider plate spacing (16 inches) than the units that formed the basis for Southern Research Institutes original algorithms for which the widest spacing was 12 inches and most of the data were for ESP's with 9-inch plate spacing. While it is not known how this might affect the results, it appears that the algorithms in *ESPert* underestimate the operating conditions -- secondary voltage and current -- and therefore underestimate the performance. Additional data from ESPs with wide plate spacing should be incorporated into the *ESPert* model to expand its capabilities.

Air load curves should not be used to predict the operating point for a TR set with high dust loading. For both sides of the ESP, TR Set 1 exhibited full load secondary operating current and voltage that were much higher than the air load curves. Empirical adjustment of the air load curves to account for this shift, improved the estimates of the ESP effectiveness.

References

1. "ESP Modifications at NYSEG's Milliken Station Units 1 and 2", Marker, B. L. and Beckman, E. G., *Joint ASME/IEEE Power Generation Conference*, Kansas City, Kansas, October 17-22, 1993.
2. DeVito, M. S.; Oda, R. L.; Marker, B. *Milliken Clean Coal Technology Demonstration Project, Unit 2 Electrostatic Precipitator Upgrade Performance Testing, Interim Report*, a report to New York State Electric & Gas Corporation, November 1995.
3. Electric Power Research Institute, *ESPert™*)) *Electrostatic Precipitator Performance Diagnostic Model*, EPRI TR-104690, User's Manual, December 1994.
4. Electric Power Research Institute, *Precipitator Performance Estimation Procedure*, EPRI CS-5040, February 1987.

Figure 1

Measured & Predicted Ash Resistivities

NYSEG's Milliken Station, Oct. 1995

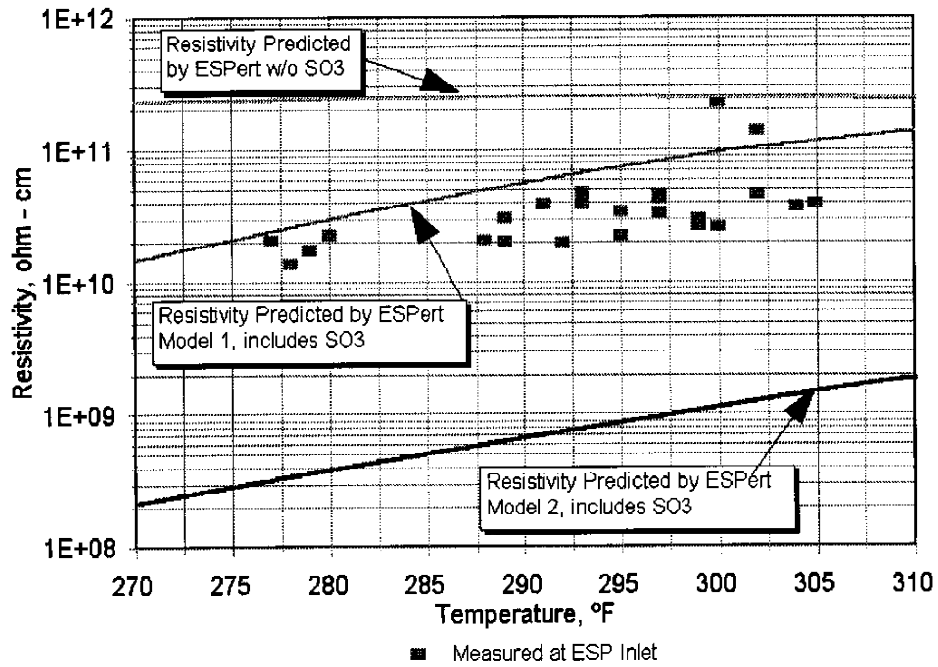


Figure 2

Position and Measured Ash Resistivity

NYSEG's Milliken Station, Oct. 1995

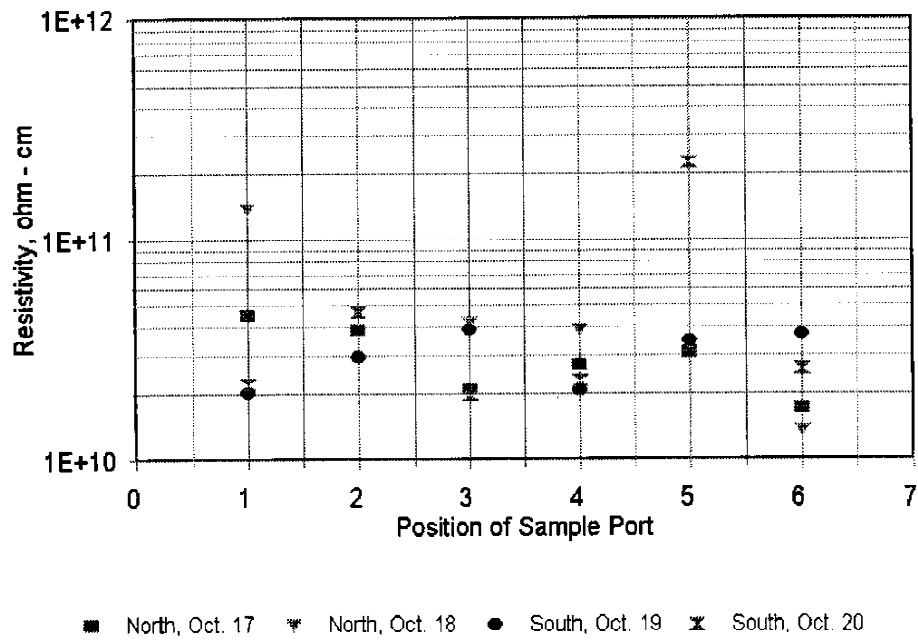


Figure 3

Operational Parameters
NYSEG's Milliken Station, Oct. 1995

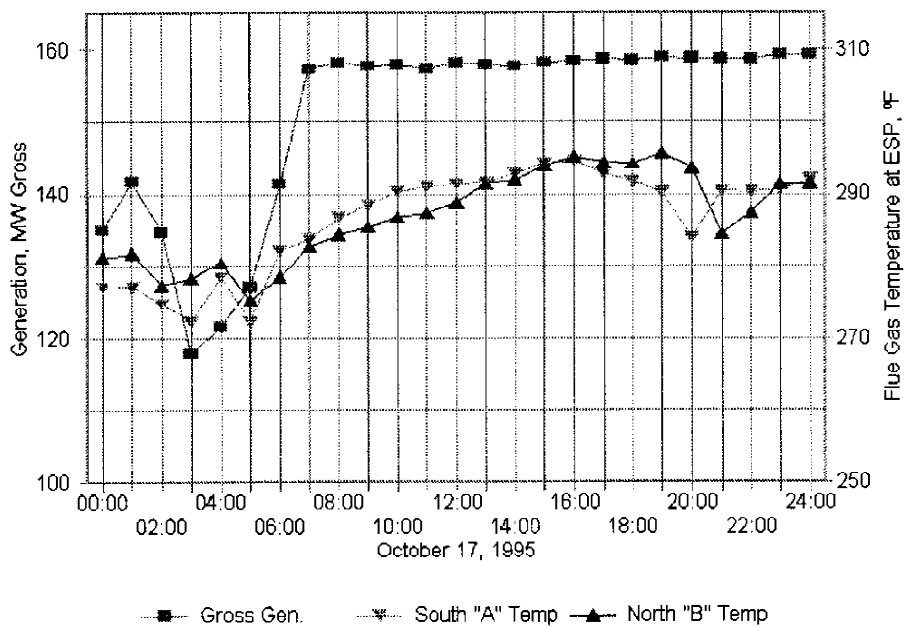


Figure 4

Operational Parameters
NYSEG's Milliken Station, Oct. 1995

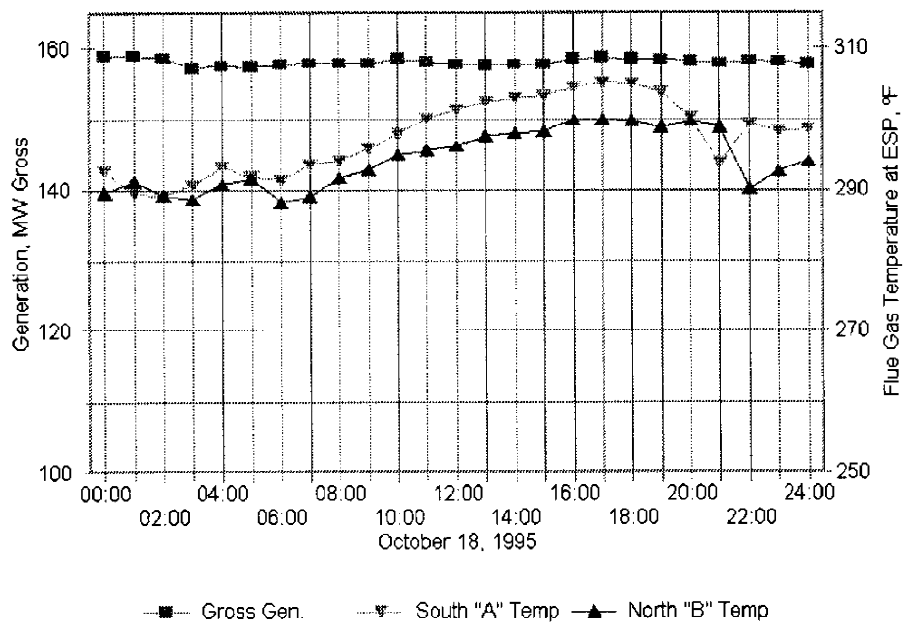


Figure 5

Operational Parameters
NYSEG's Milliken Station, Oct. 1995

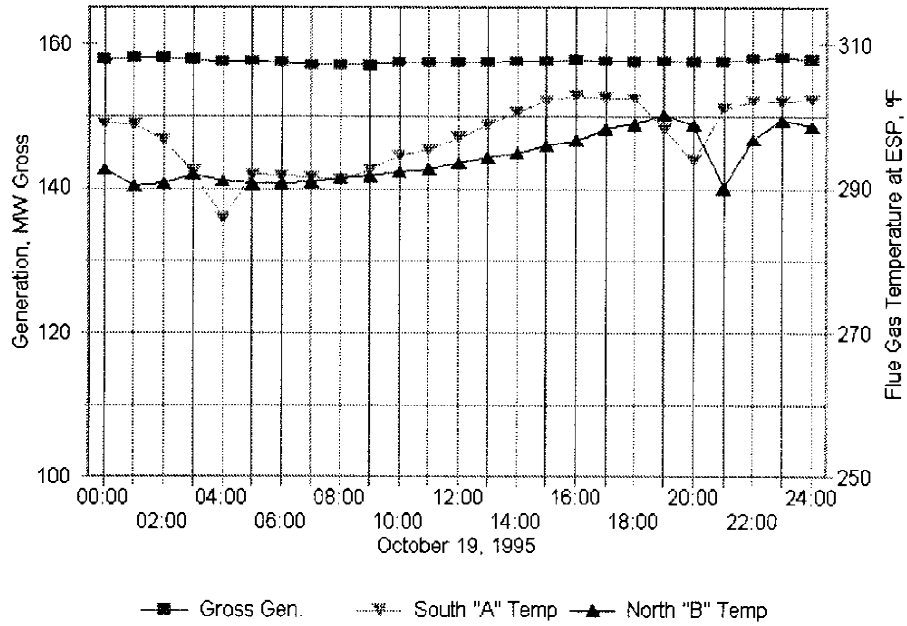


Figure 6

Operational Parameters
NYSEG's Milliken Station, Oct. 1995

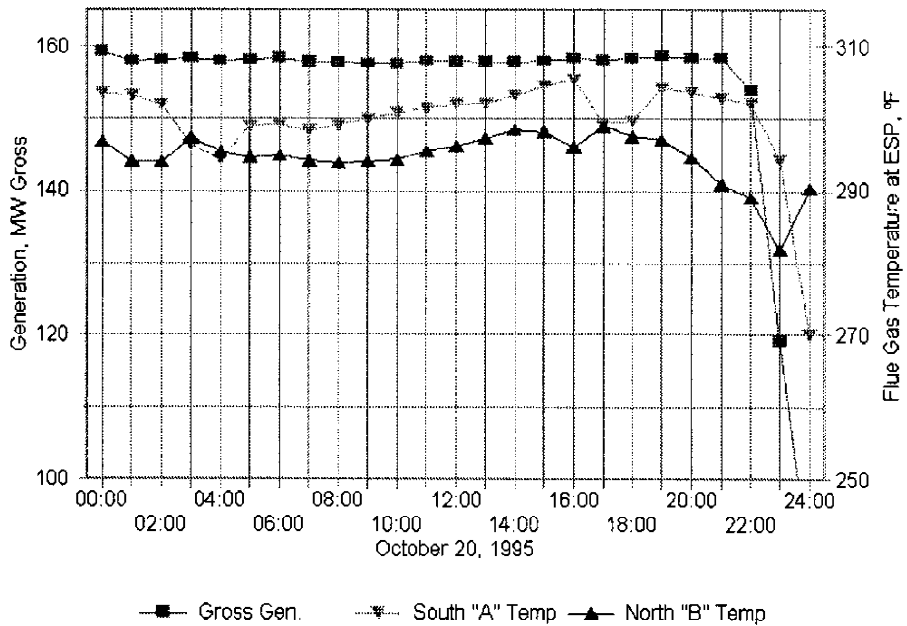


Figure 7
V-I Readings for TR Set 2-B1
 NYSEG's Milliken Station, Oct. 1995

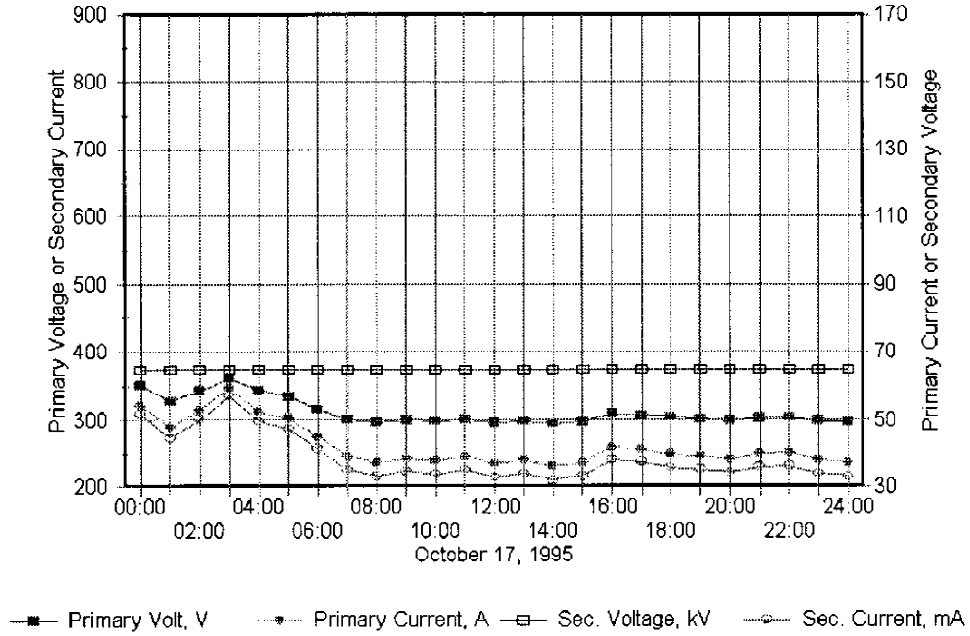


Figure 8
V-I Readings for TR Set 2-B2
 NYSEG's Milliken Station, Oct. 1995

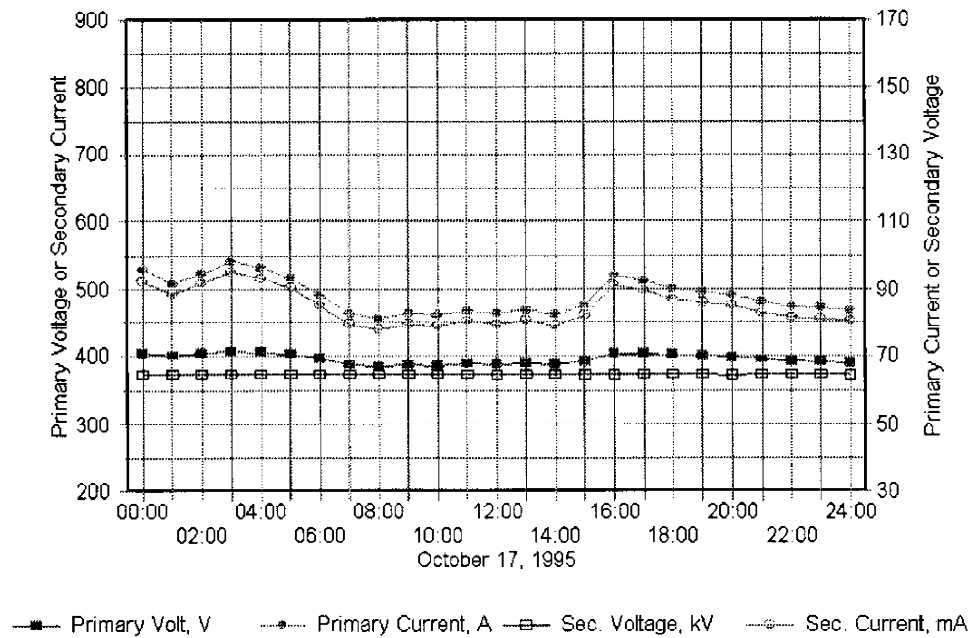


Figure 9
V-I Readings for TR Set 2-B3
 NYSEG's Milliken Station, Oct. 1995

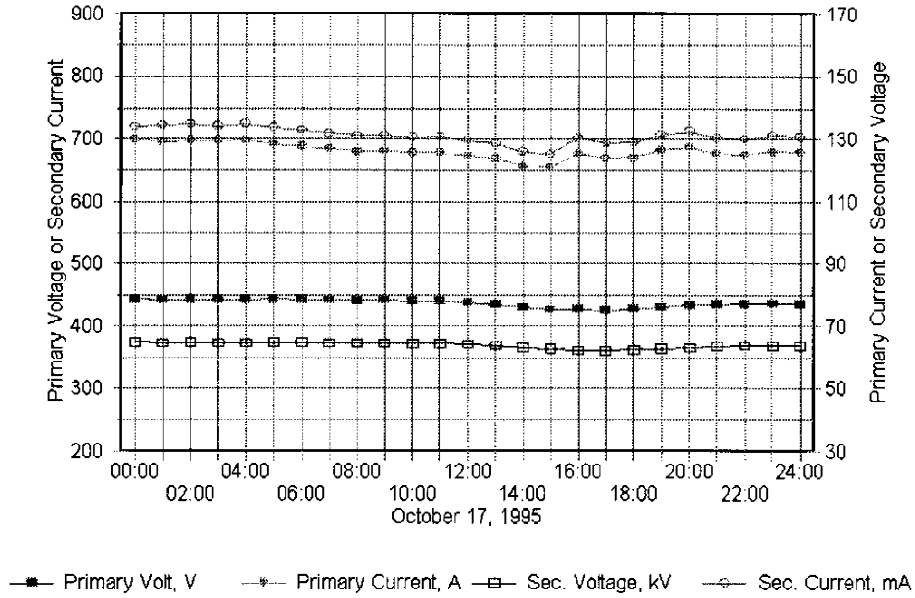


Figure 10
V-I Readings for TR Set 2-B1
 NYSEG's Milliken Station, Oct. 1995

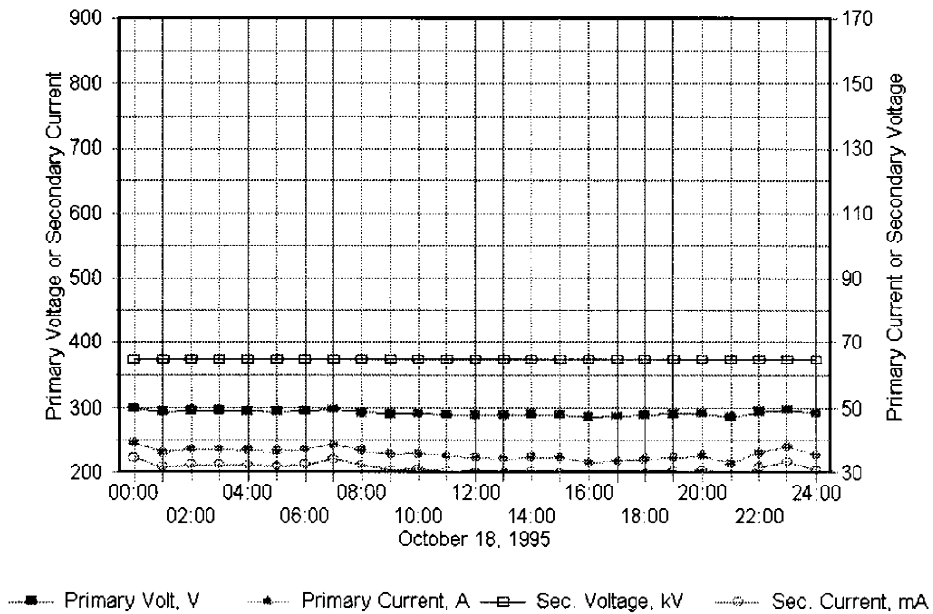


Figure 11
V-I Readings for TR Set 2-B2
 NYSEG's Milliken Station, Oct. 1995

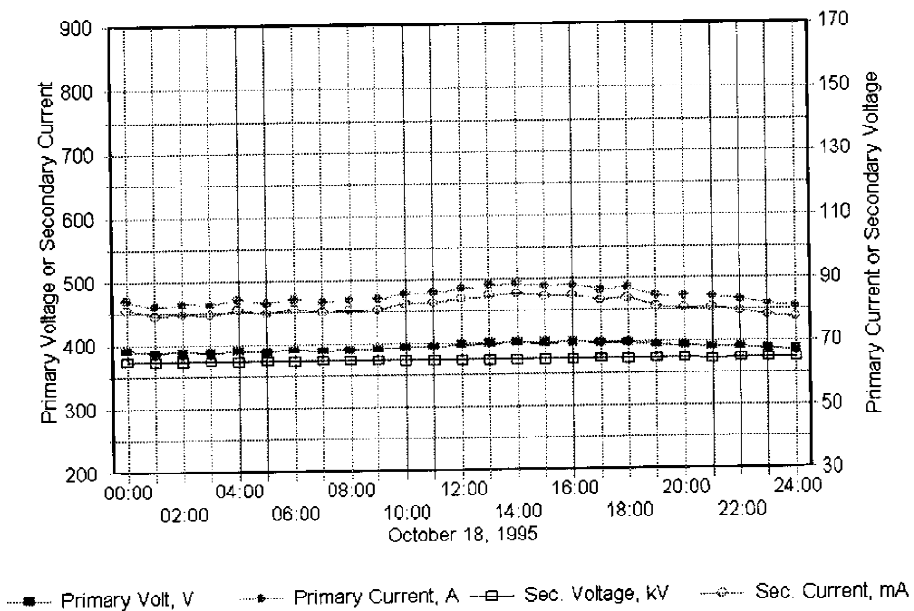


Figure 12
V-I Readings for TR Set 2-B3
 NYSEG's Milliken Station, Oct. 1995

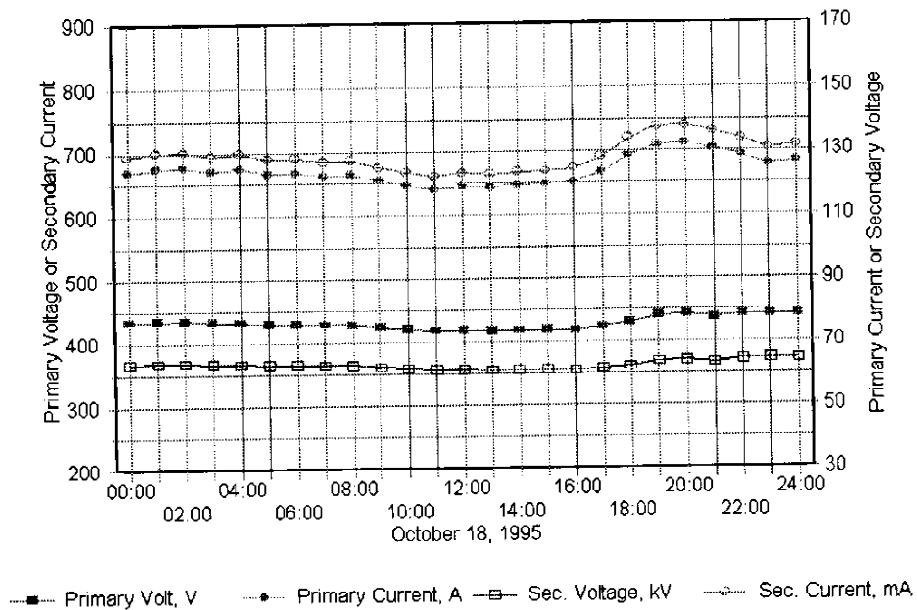


Figure 13
V-I Readings for TR Set 2-A1
 NYSEG's Milliken Station, Oct. 1995

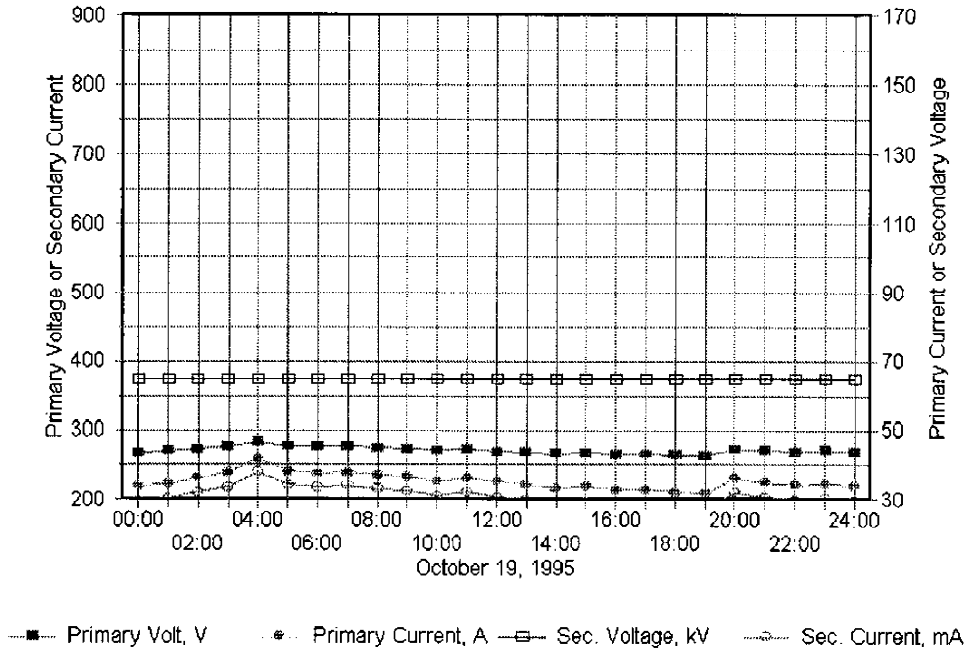


Figure 14
V-I Readings for TR Set 2-A2
 NYSEG's Milliken Station, Oct. 1995

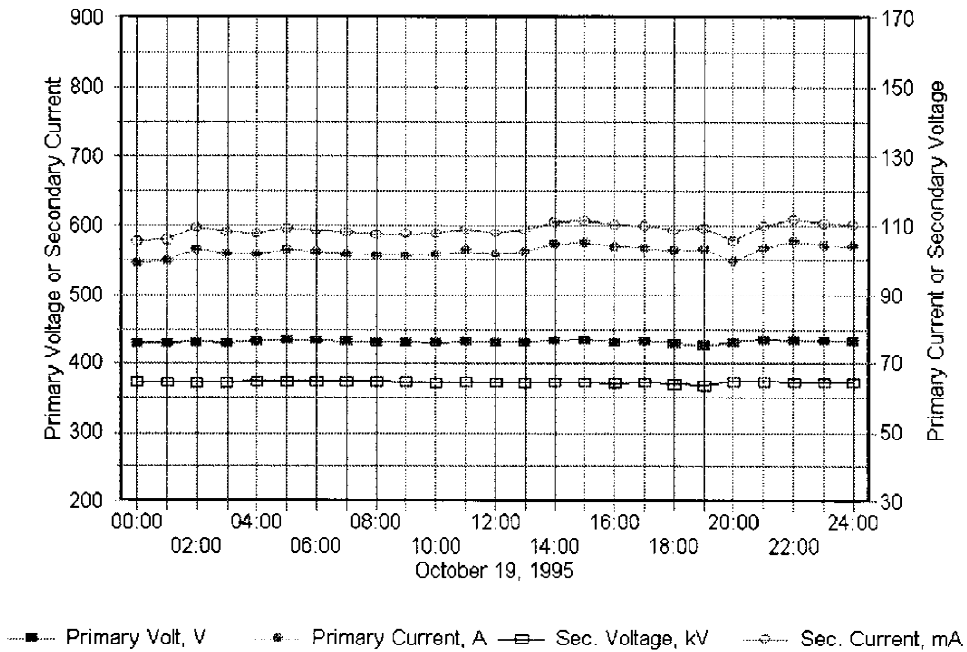


Figure 15
V-I Readings for TR Set 2-A3
 NYSEG's Milliken Station, Oct. 1995

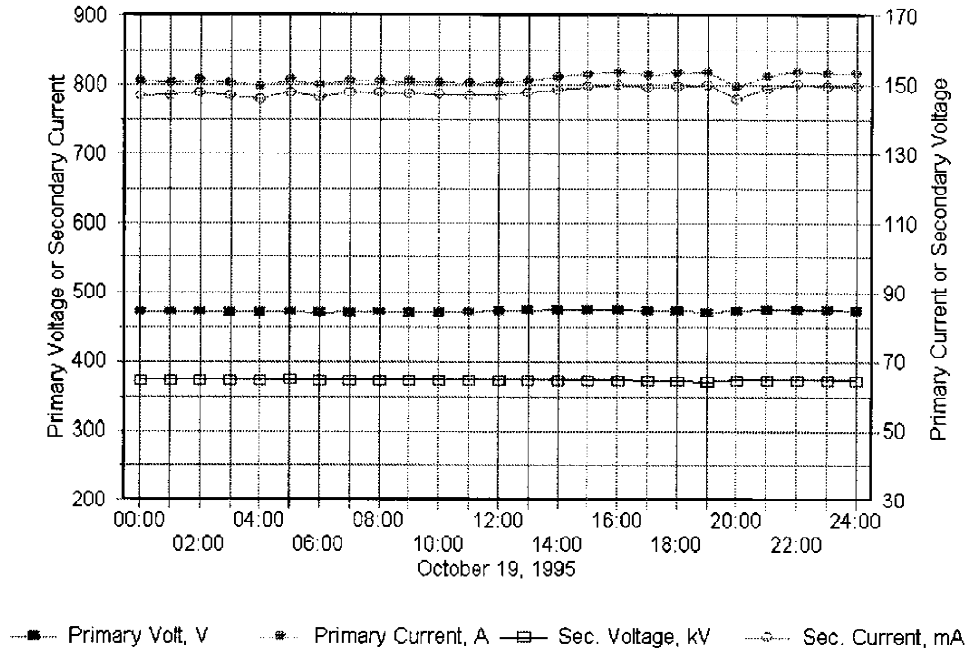


Figure 16
V-I Readings for TR Set 2-A1
 NYSEG's Milliken Station, Oct. 1995

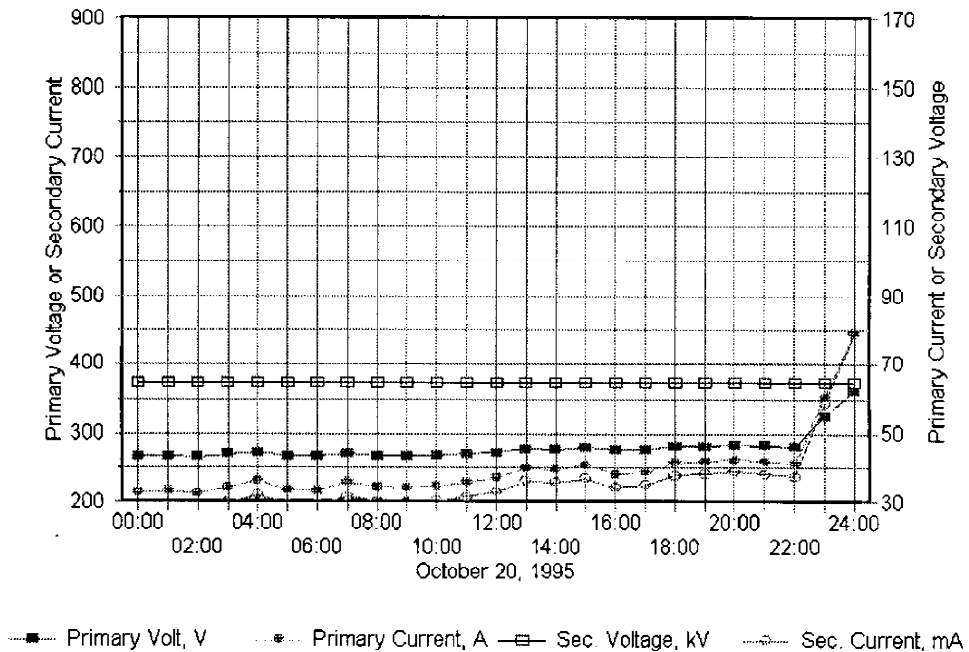


Figure 17
V-I Readings for TR Set 2-A2
 NYSEG's Milliken Station, Oct. 1995

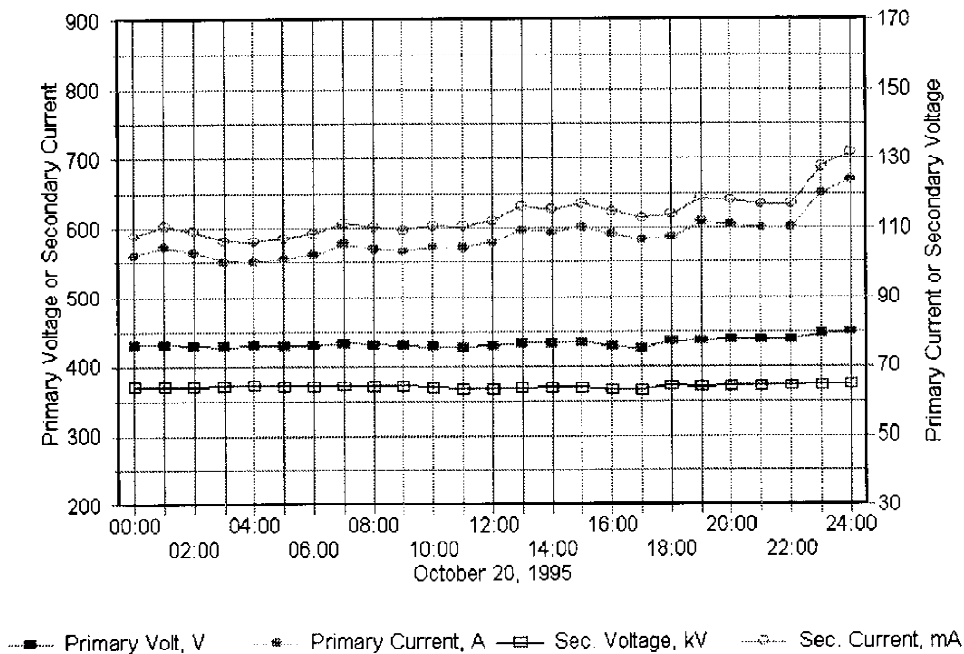


Figure 18

V-I Readings for TR Set 2-A3
 NYSEG's Milliken Station, Oct. 1995

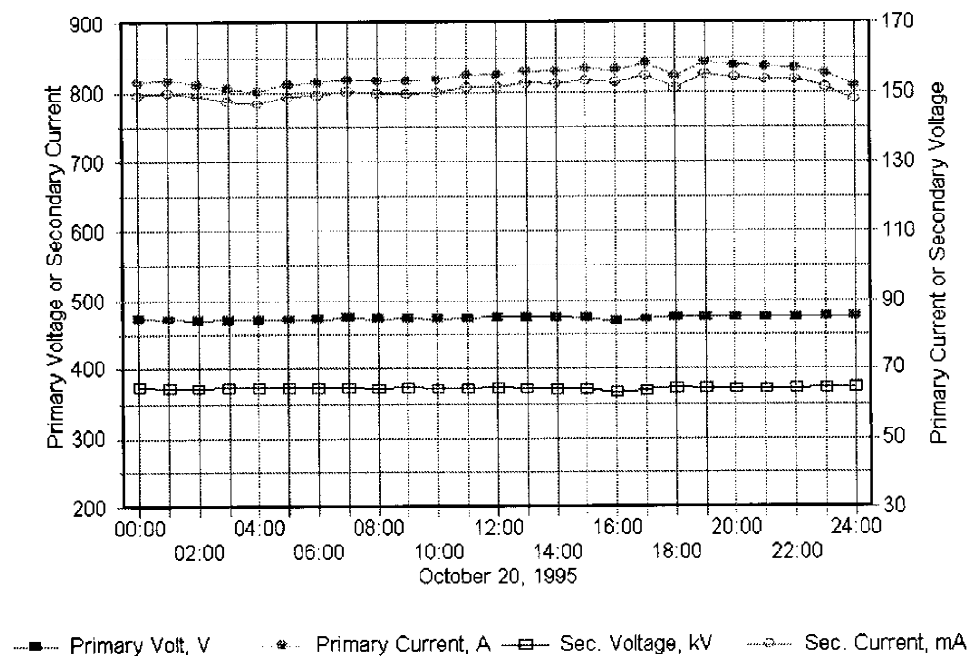


Figure 19

Rosin-Rammler Plot - North ESP Data
 NYSEG's Milliken Station, Oct. 1995

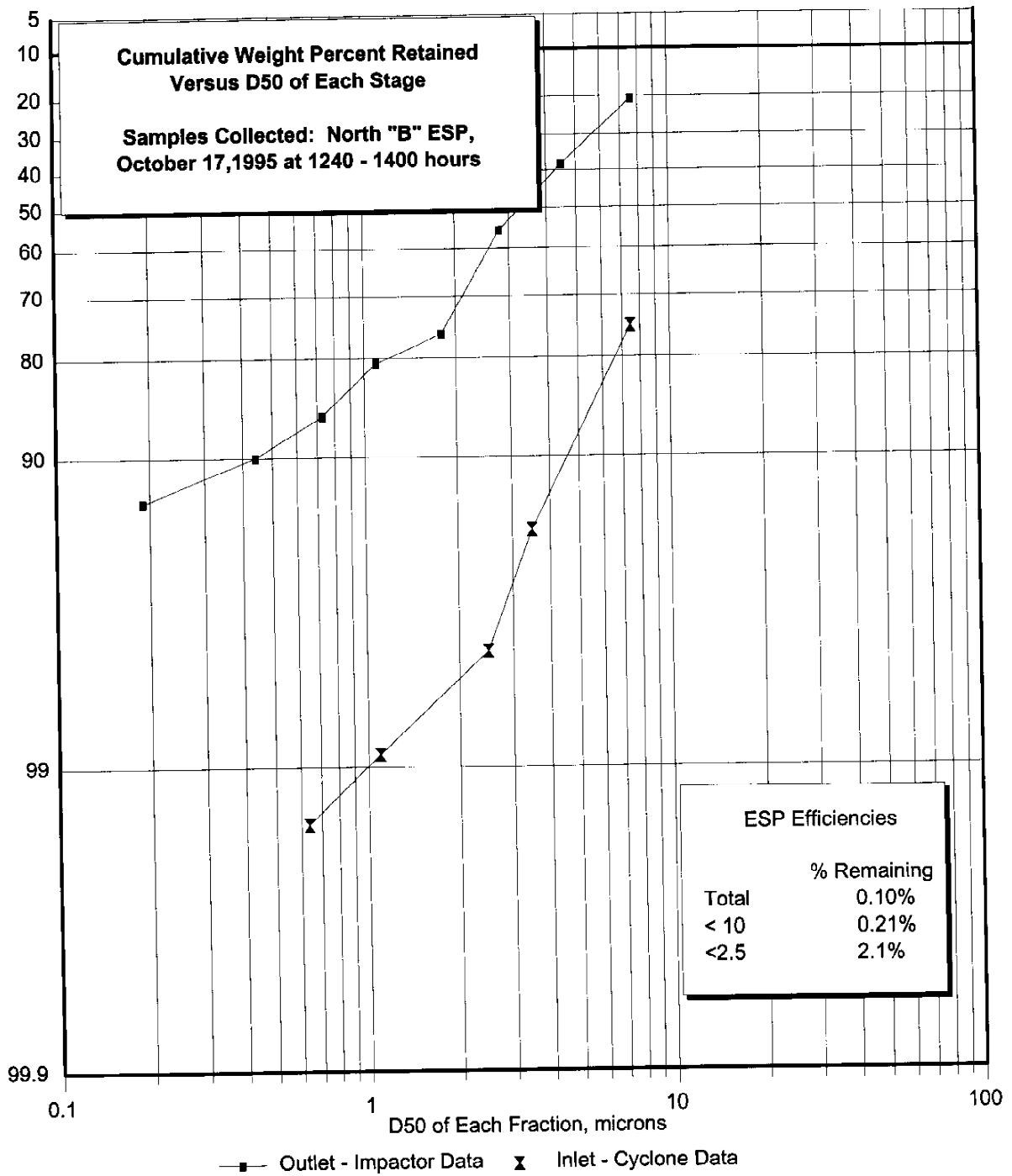


Figure 20

Rosin-Rammler Plot - North ESP Data

NYSEG's Milliken Station, Oct. 1995

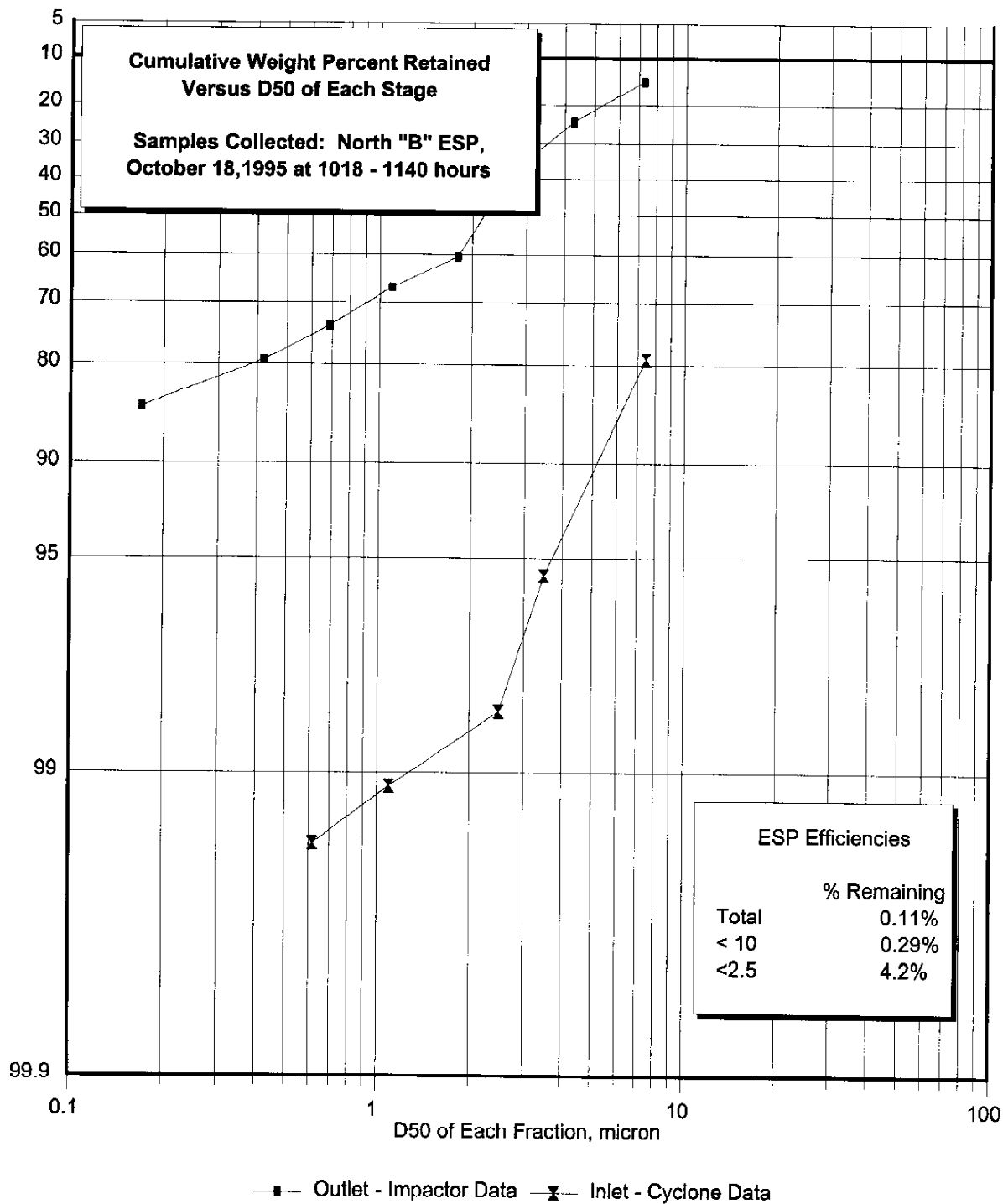


Figure 21

Rosin-Rammler Plot - South ESP Data
 NYSEG's Milliken Station, Oct. 1995

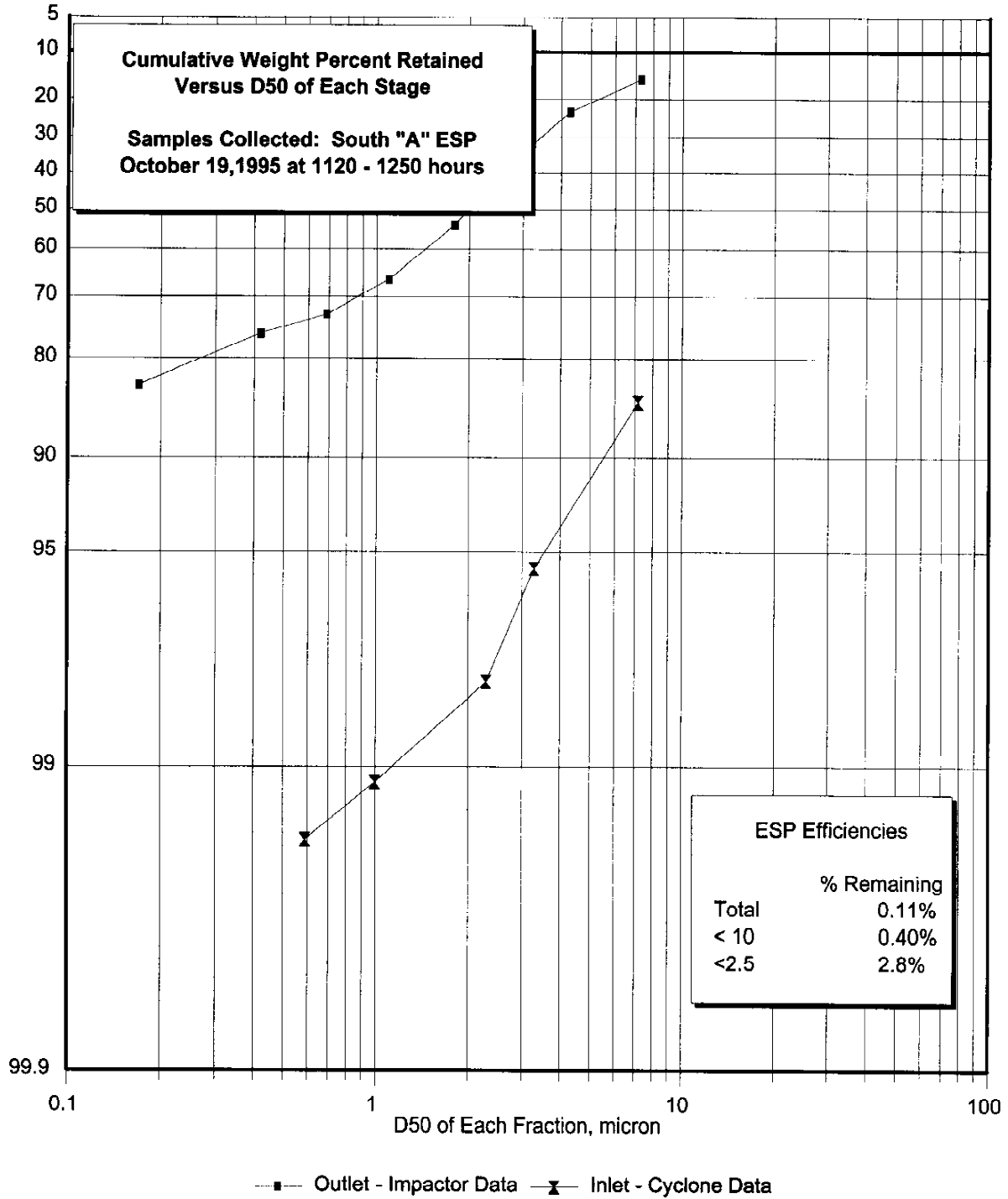


Figure 22

Rosin-Rammler Plot - South ESP Data

NYSEG's Milliken Station, Oct. 1995

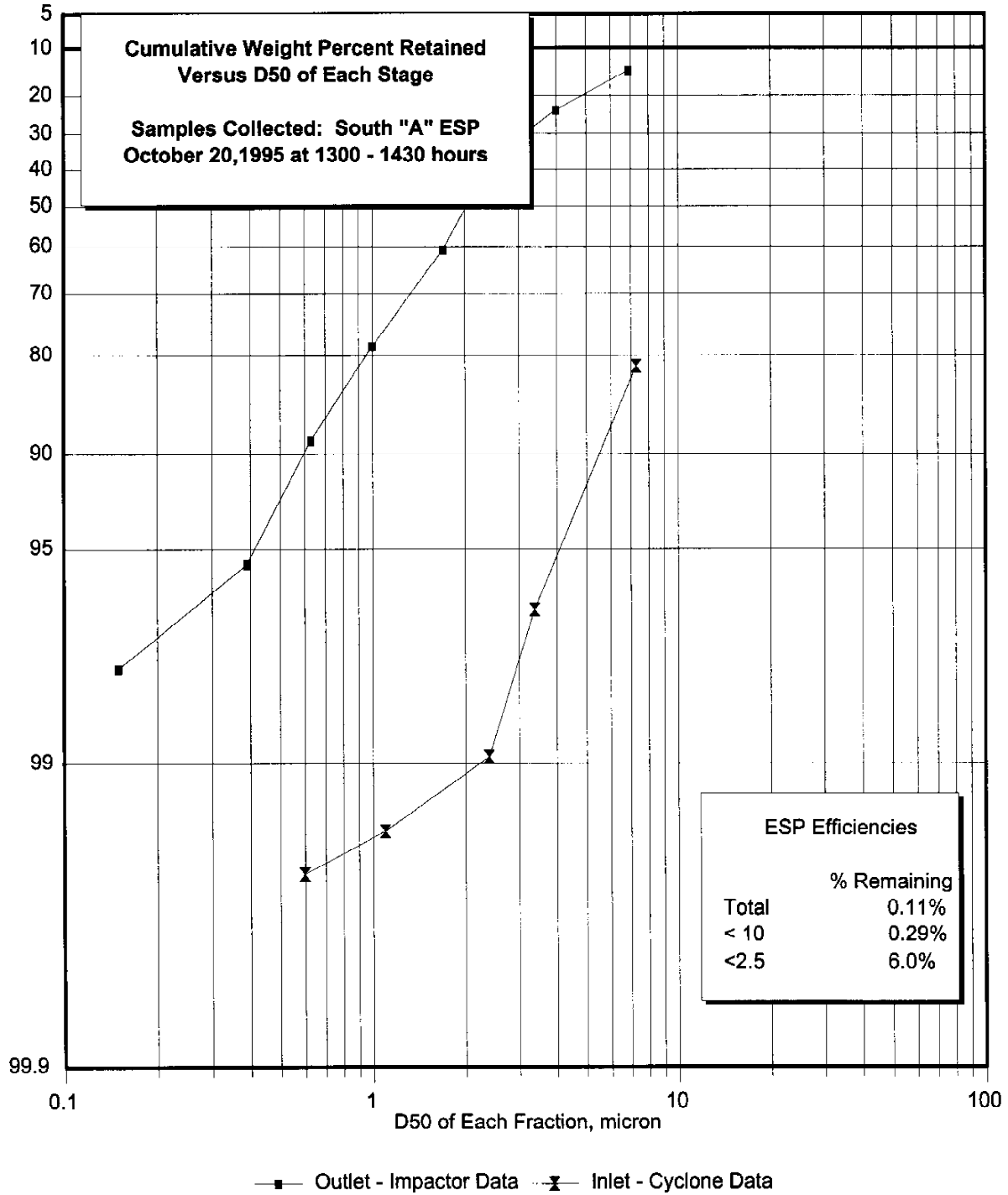


Figure 23

Rosin-Rammler Plot - Combined Inlet
NYSEG's Milliken Station, Oct. 1995

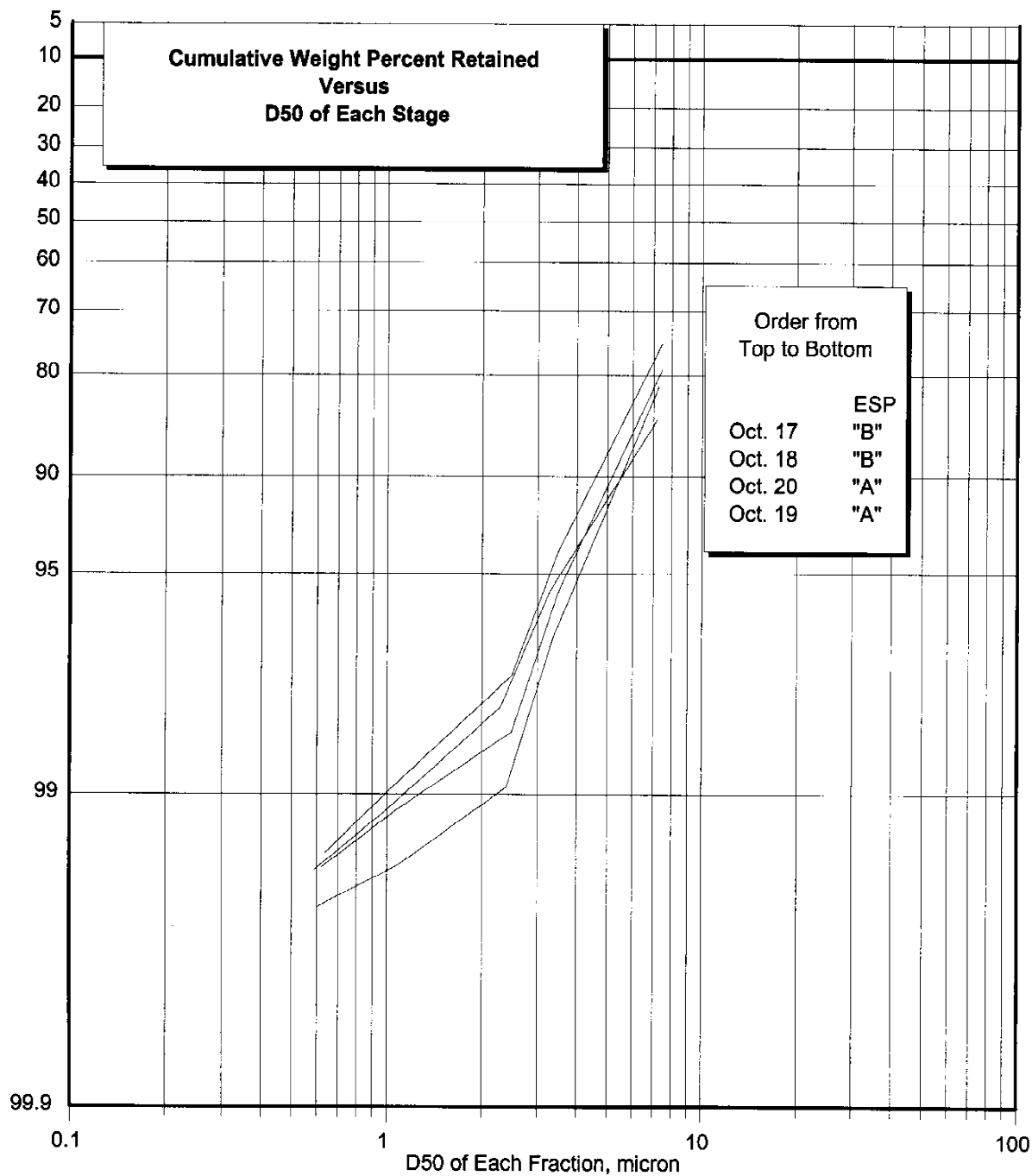


Figure 24

Rosin-Rammler Plot - ESP Exit
NYSEG's Milliken Station, Oct. 1995

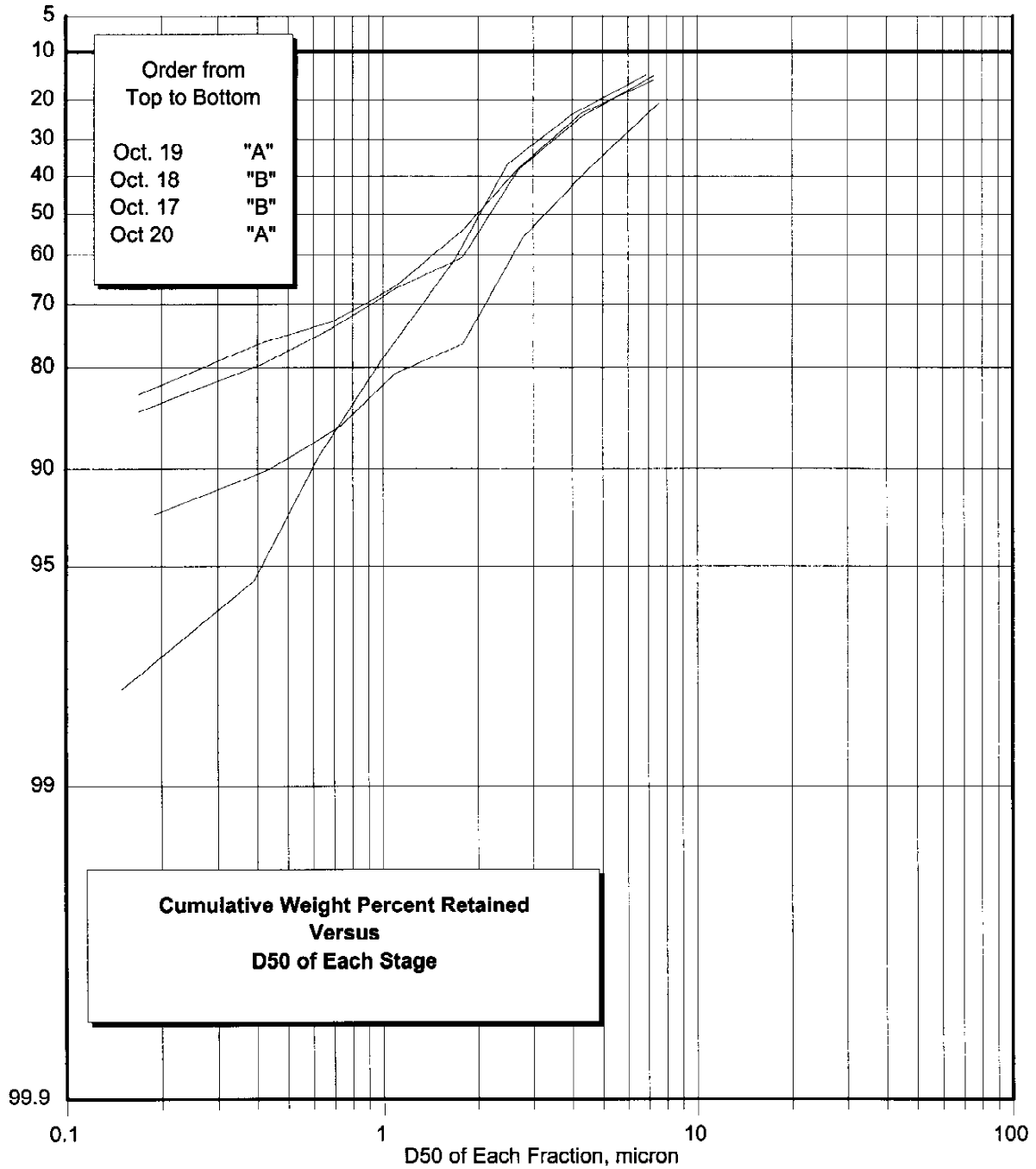
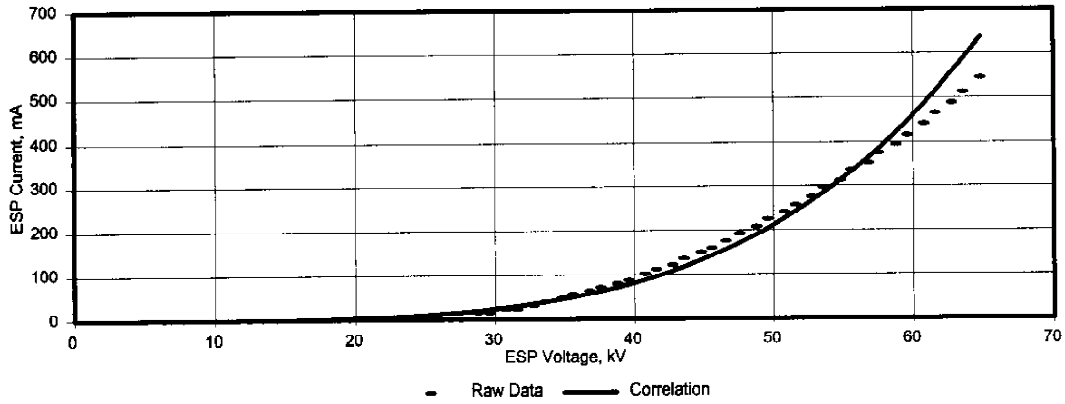
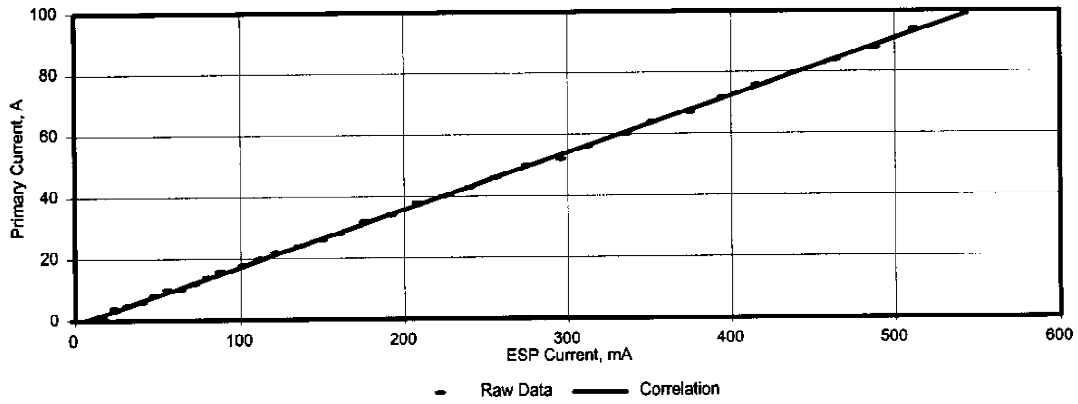


Figure 25

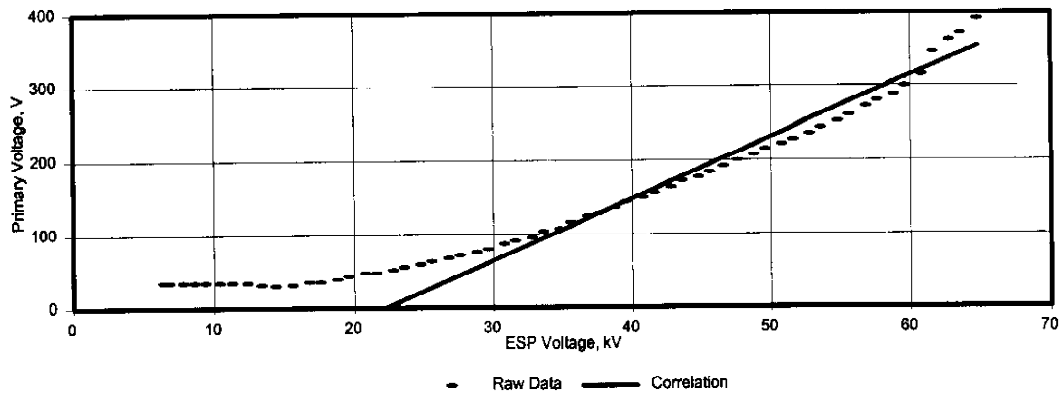
TR Set 2-A1 Air Load Test Data Correlation for ESPert
NYSEG's Milliken Station, March 1996



$$\text{ESP Voltage (KV)} = 14.3 \times \text{ESP Current (mA)}^{0.234}$$



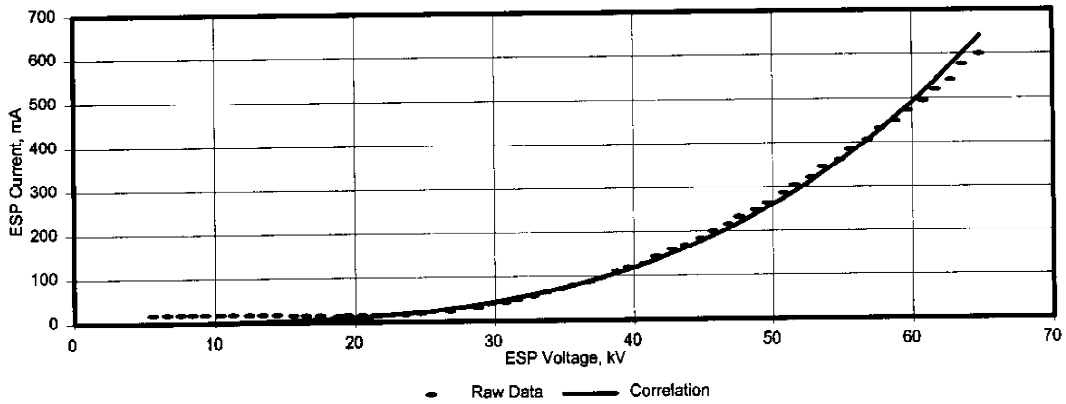
$$\text{Primary Current (A)} = -1.12 + 0.184 \times \text{ESP Current (mA)}$$



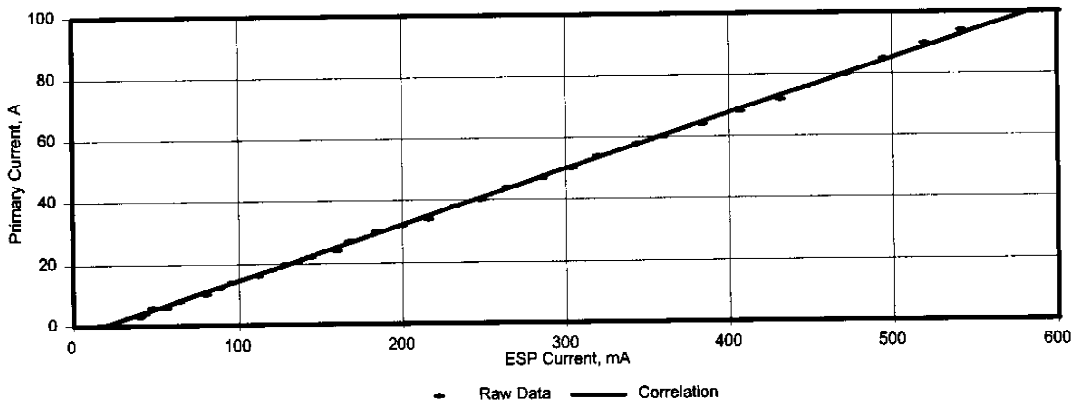
$$\text{Primary Voltage (V)} = -186 + 8.34 \times \text{ESP Voltage (kV)}$$

Figure 26

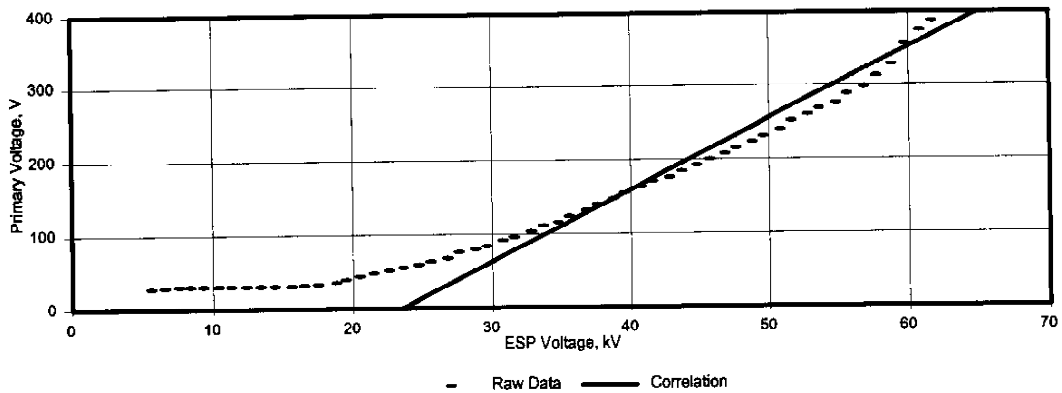
TR Set 2-A2 Air Load Test Data Correlation for ESPert
NYSEG's Milliken Station, March 1996



$$\text{ESP Voltage (KV)} = 10.2 \times \text{ESP Current (mA)}^{0.288}$$



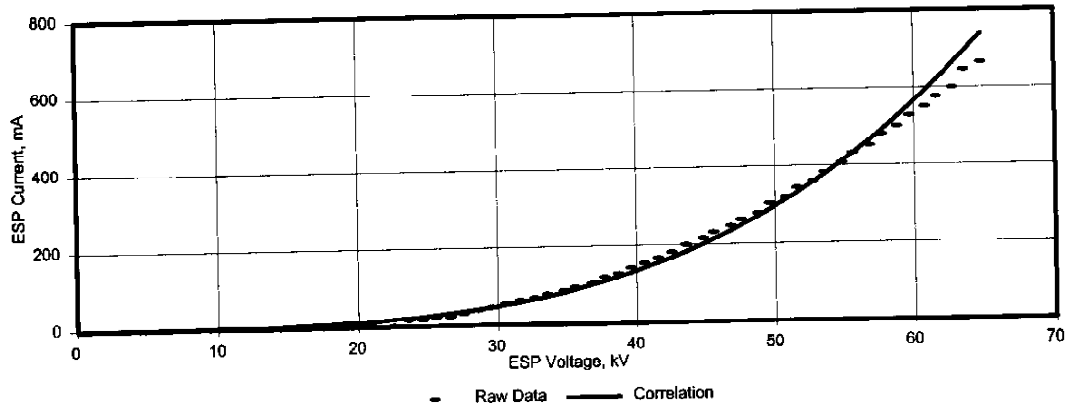
$$\text{Primary Current (A)} = -3.21 + 0.177 \times \text{ESP Current (mA)}$$



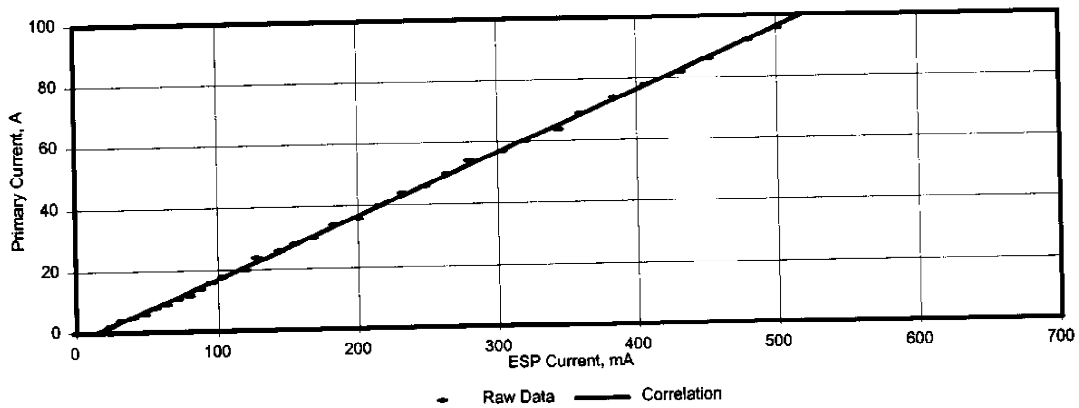
$$\text{Primary Voltage (V)} = -227 + 9.65 \times \text{ESP Voltage (kV)}$$

Figure 27

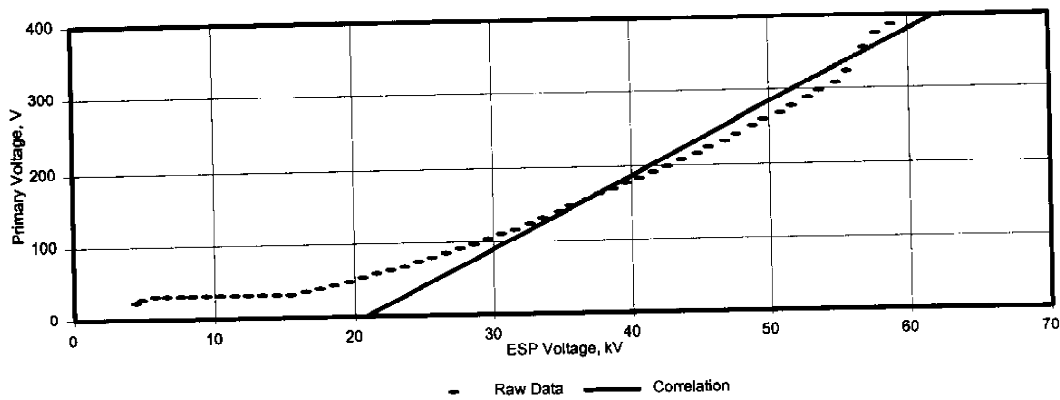
**TR Set 2-A3 Air Load Test Data Correlation for ESPert
NYSEG's Milliken Station, March 1996**



$$\text{ESP Voltage (KV)} = 10.0 \times \text{ESP Current (mA)}^{0.283}$$



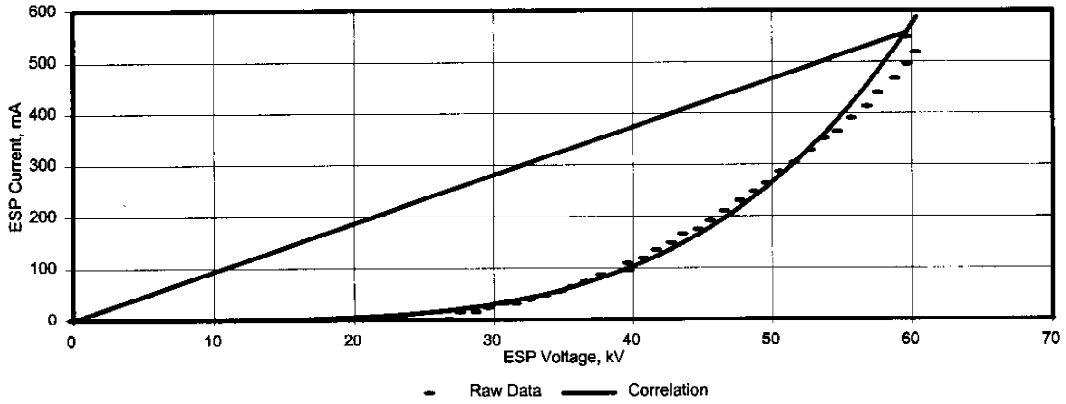
$$\text{Primary Current (A)} = -2.83 + 0.198 \times \text{ESP Current (mA)}$$



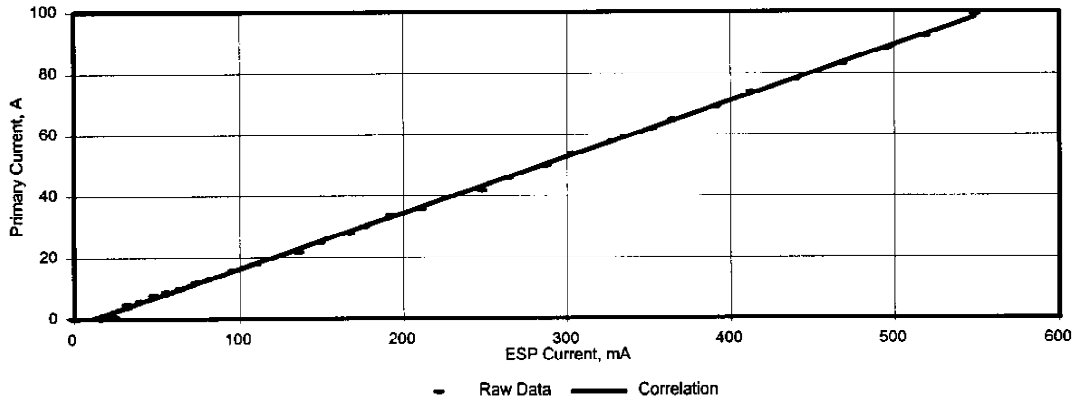
$$\text{Primary Voltage (V)} = -202 + 9.71 \times \text{ESP Voltage (kV)}$$

Figure 28

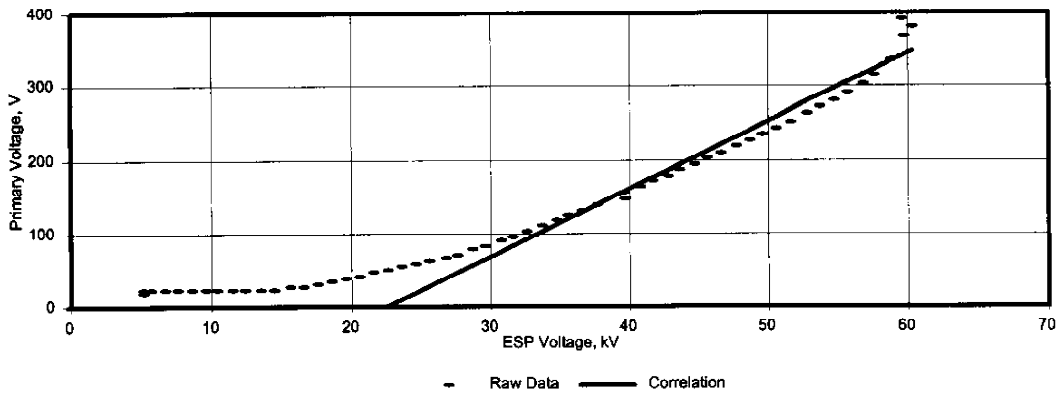
TR Set 2-B1 Air Load Test Data Correlation for ESPert
NYSEG's Milliken Station, March 1996



$$\text{ESP Voltage (KV)} = 13.4 \times \text{ESP Current (mA)}^{0.236}$$



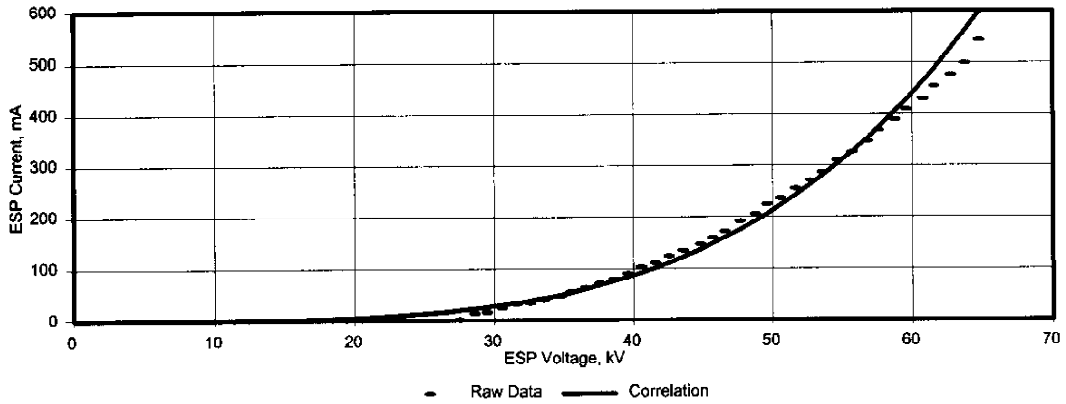
$$\text{Primary Current (A)} = -1.86 + 0.182 \times \text{ESP Current (mA)}$$



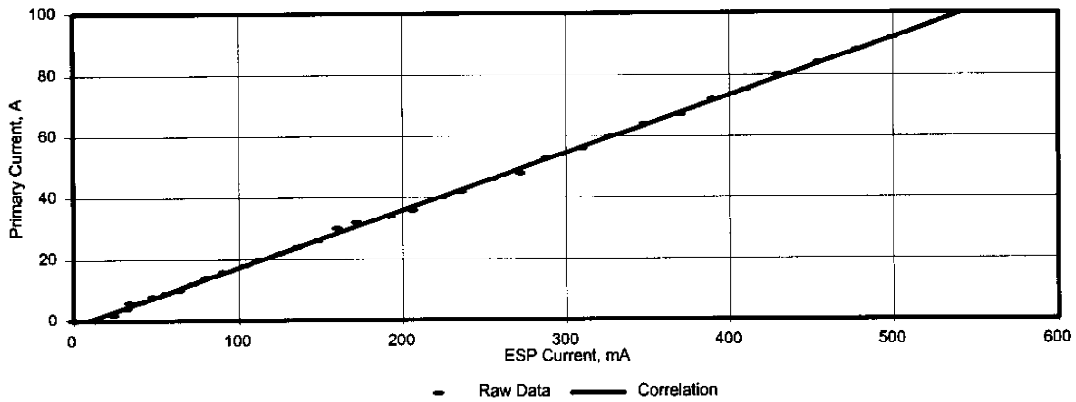
$$\text{Primary Voltage (V)} = -207 + 9.20 \times \text{ESP Voltage (kV)}$$

Figure 29

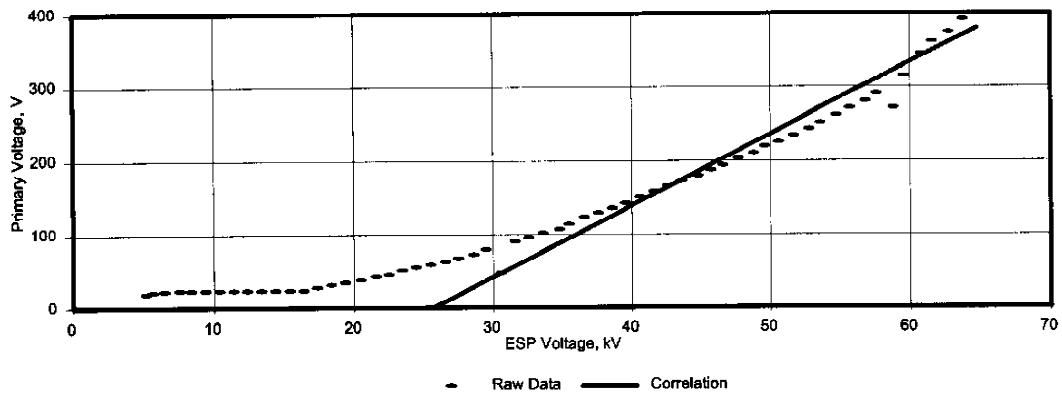
TR Set 2-B2 Air Load Test Data Correlation for ESPert
NYSEG's Milliken Station, March 1996



$$\text{ESP Voltage (KV)} = 13.1 \times \text{ESP Current (mA)}^{0.250}$$



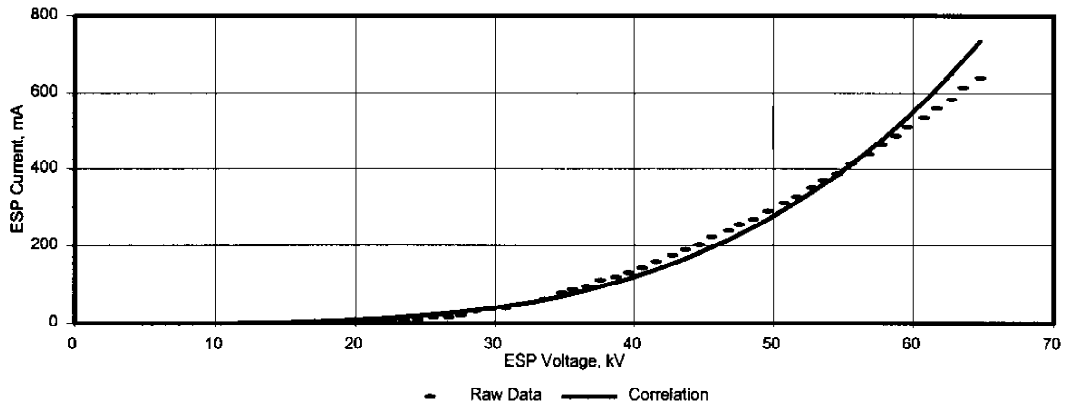
$$\text{Primary Current (A)} = -1.50 + 0.187 \times \text{ESP Current (mA)}$$



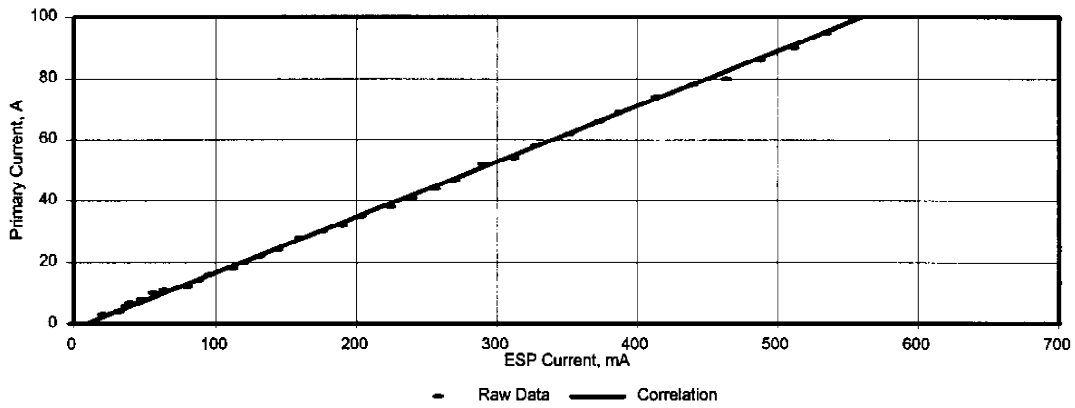
$$\text{Primary Voltage (V)} = -250 + 9.72 \times \text{ESP Voltage (kV)}$$

Figure 30

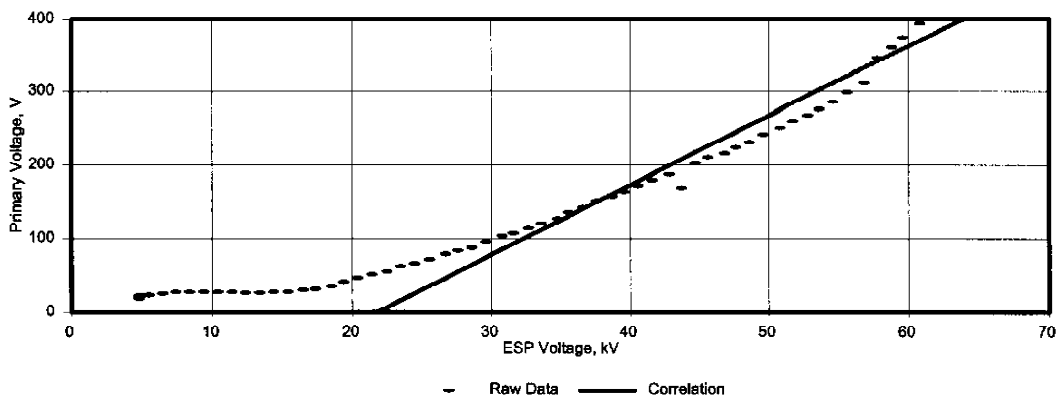
TR Set 2-B3 Air Load Test Data Correlation for ESPert
NYSEG's Milliken Station, March 1996



$$\text{ESP Voltage (KV)} = 11.2 \times \text{ESP Current (mA)}^{0.266}$$



$$\text{Primary Current (A)} = -1.54 + 0.181 \times \text{ESP Current (mA)}$$



$$\text{Primary Voltage (V)} = -207 + 9.49 \times \text{ESP Voltage (kV)}$$

Figure 31

Particulate Penetration Predictions
 NYSEG's Milliken Station, Oct. 1995

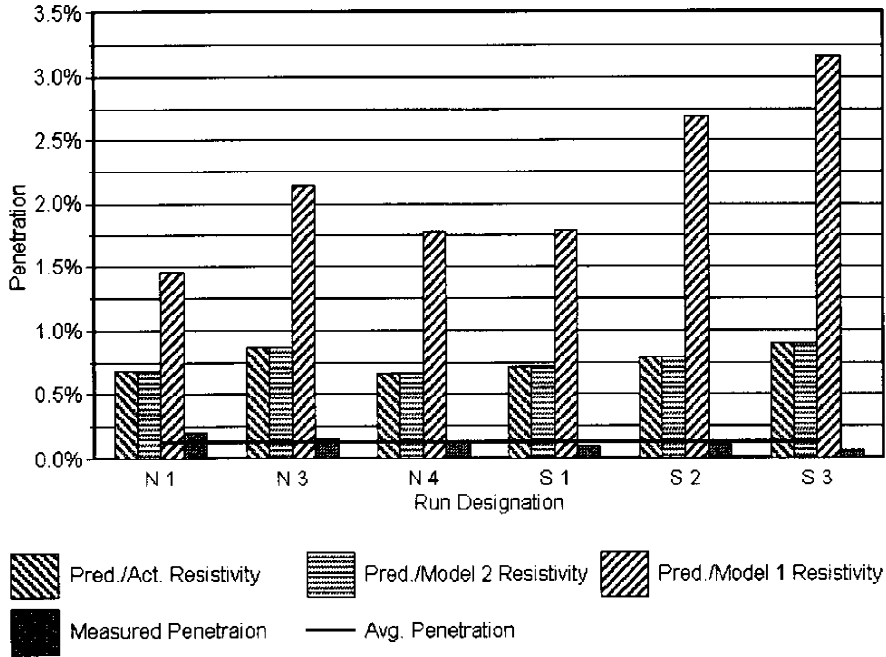


Figure 32

Minus 10 Micron Fraction Penetrations
 NYSEG's Milliken Station, Oct. 1995

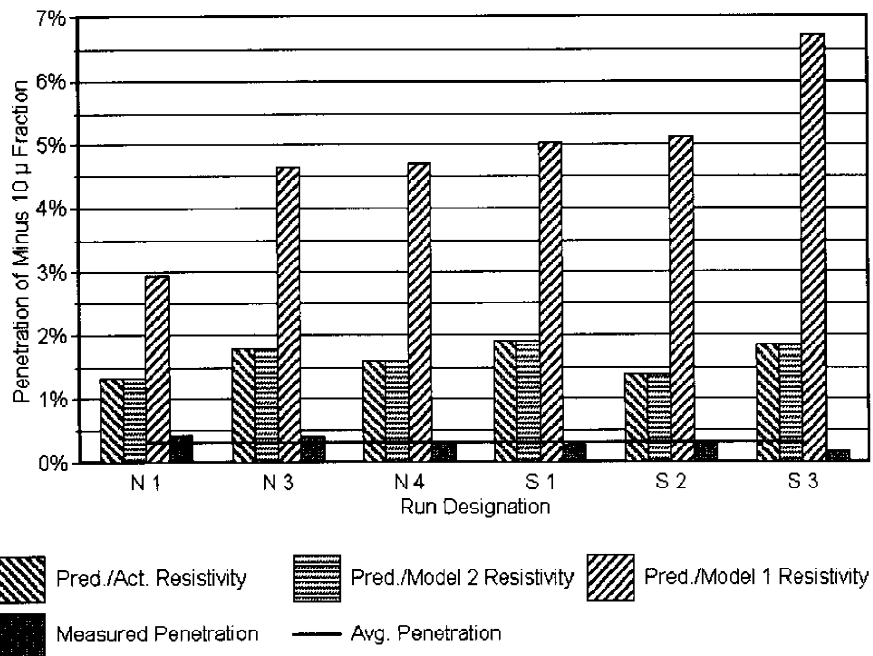


Figure 33

Minus 2.5 Micron Fraction Penetrations
NYSEG's Milliken Station, Oct. 1995

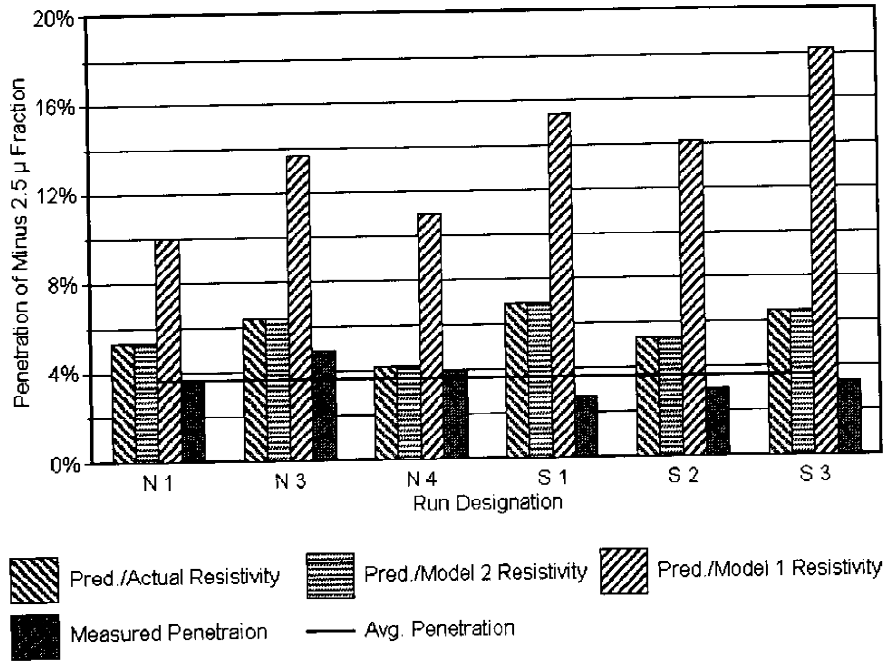
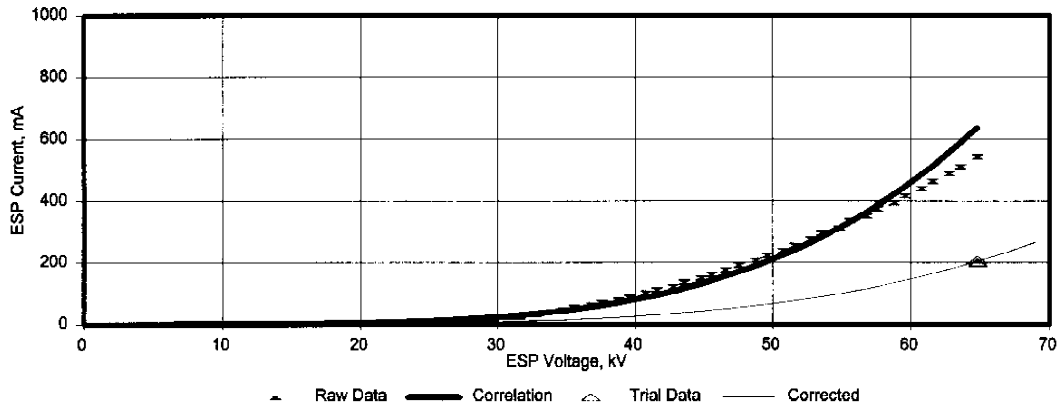
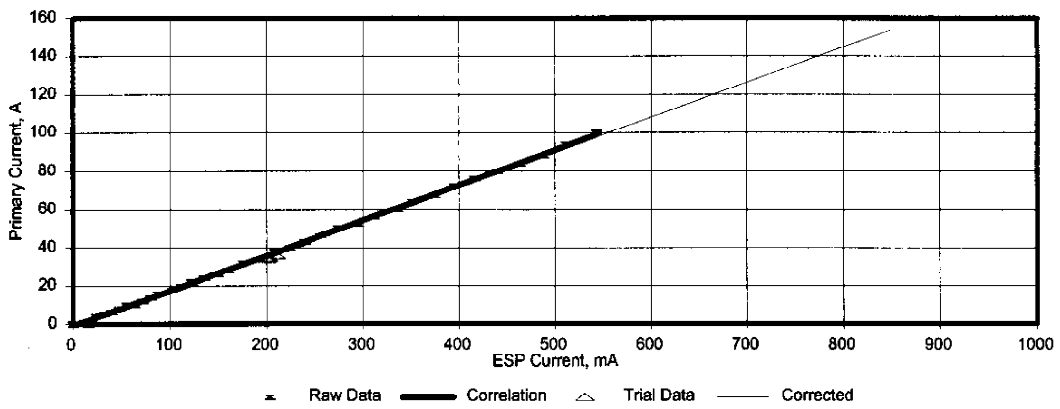


Figure 34

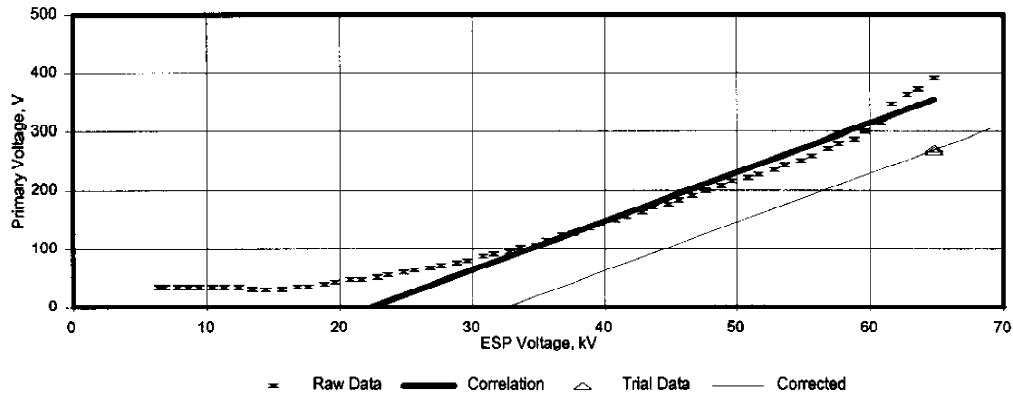
**TR Set 2-A1 Air Load Test ADJUSTED Correlation for ESPert
 NYSEG's Milliken Station, March 1996**



ADJUSTED EQUATION: ESP Voltage (KV) = 18.7 x ESP Current (mA) ^ 0.234

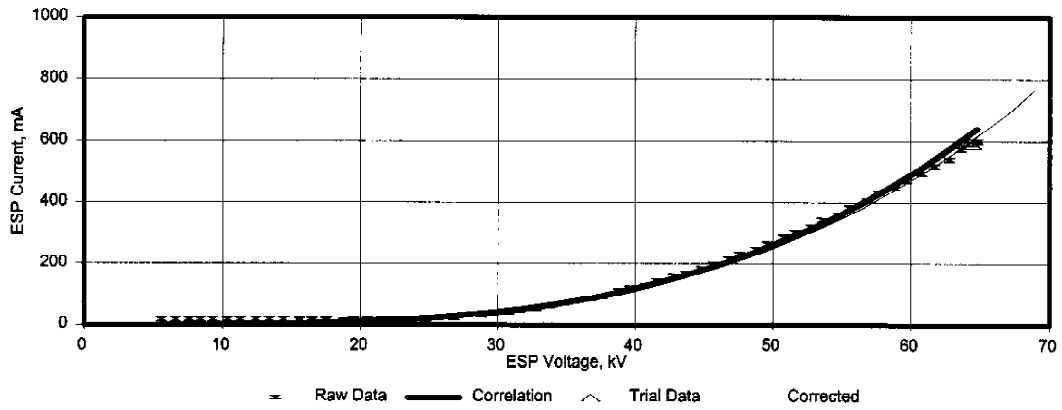


ADJUSTED EQUATION: Primary Current (A) = -2.40 + 0.184 x ESP Current (mA)

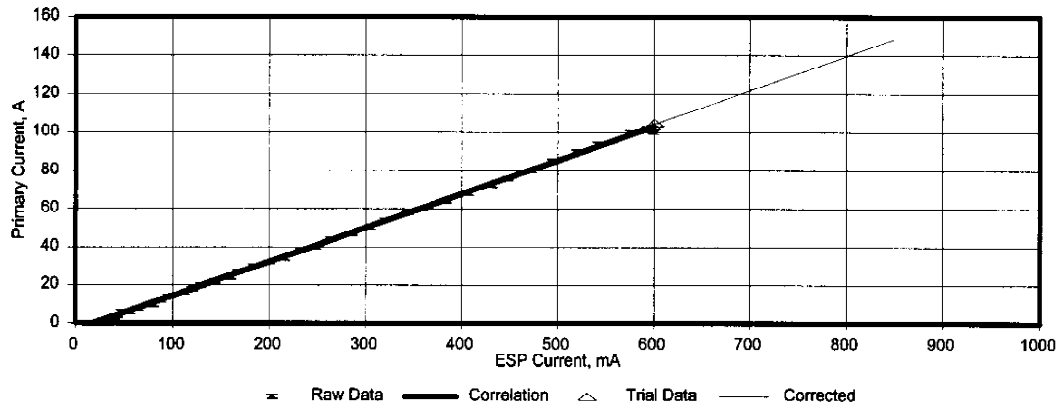


ADJUSTED EQUATION: Primary Voltage (V) = -271 + 8.34 x ESP Voltage (kV)

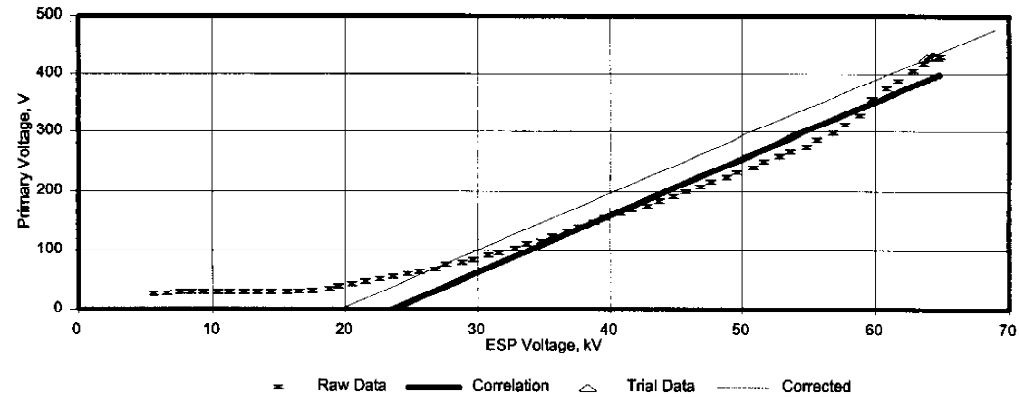
Figure 35
TR Set 2-A2 Air Load Test ADJUSTED Correlation for ESPert
 NYSEG's Milliken Station, March 1996



ADJUSTED EQUATION: ESP Voltage (KV) = 10.3 x ESP Current (mA) ^ 0.286



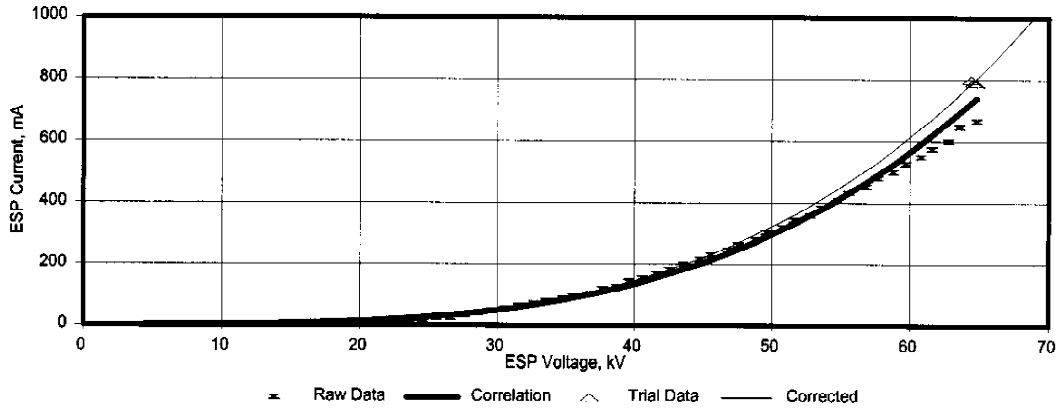
ADJUSTED EQUATION: Primary Current (A) = -2.06 + 0.177 x ESP Current (mA)



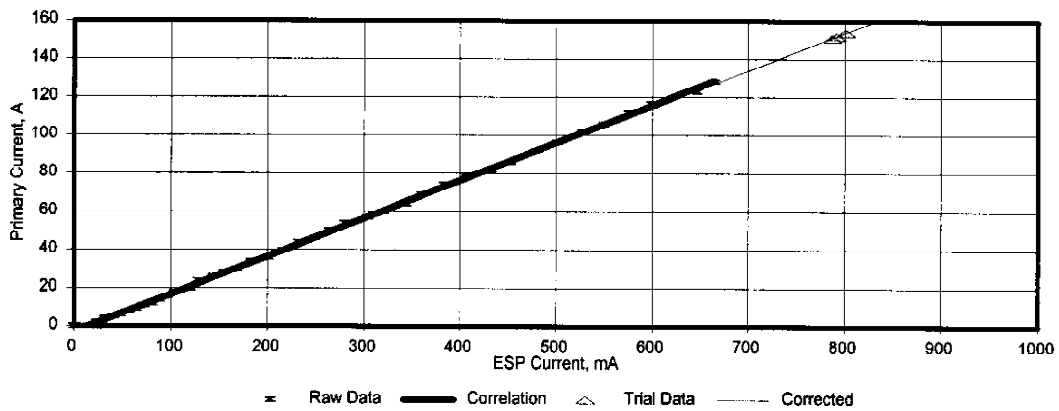
ADJUSTED EQUATION: Primary Voltage (V) = -189 + 9.65 x ESP Voltage (kV)

Figure 36

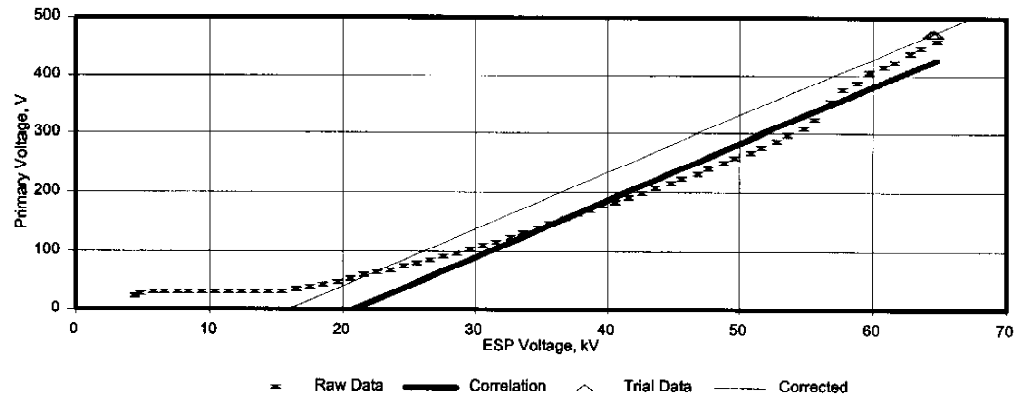
**TR Set 2-A3 Air Load Test ADJUSTED Correlation for ESPert
 NYSEG's Milliken Station, March 1996**



ADJUSTED EQUATION: ESP Voltage (KV) = 9.8 x ESP Current (mA) ^ 0.283



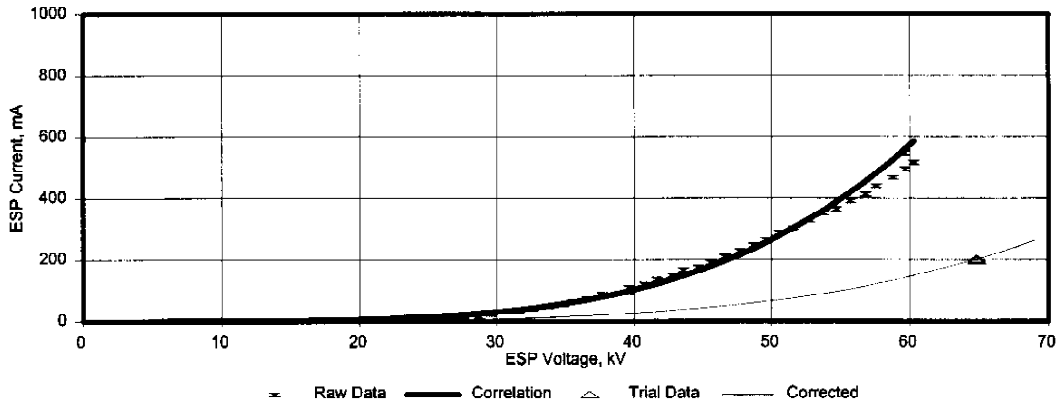
ADJUSTED EQUATION: Primary Current (A) = -4.88 + 0.198 x ESP Current (mA)



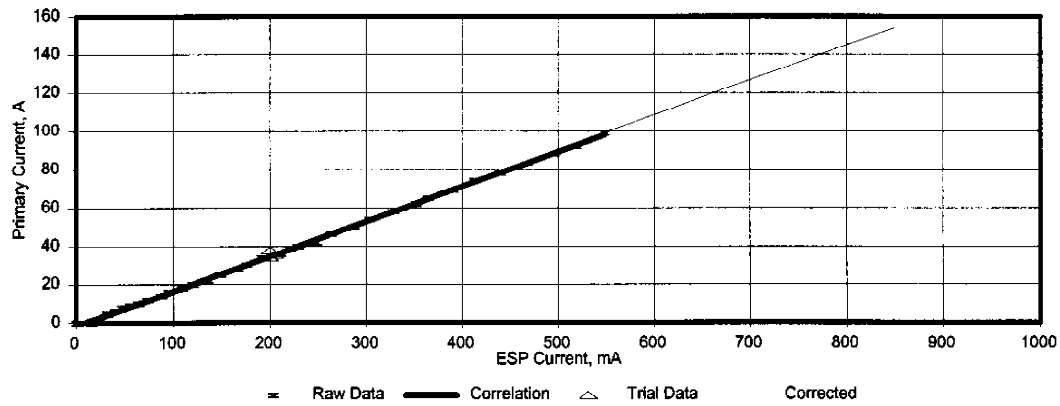
ADJUSTED EQUATION: Primary Voltage (V) = -154 + 9.71 x ESP Voltage (kV)

Figure 37

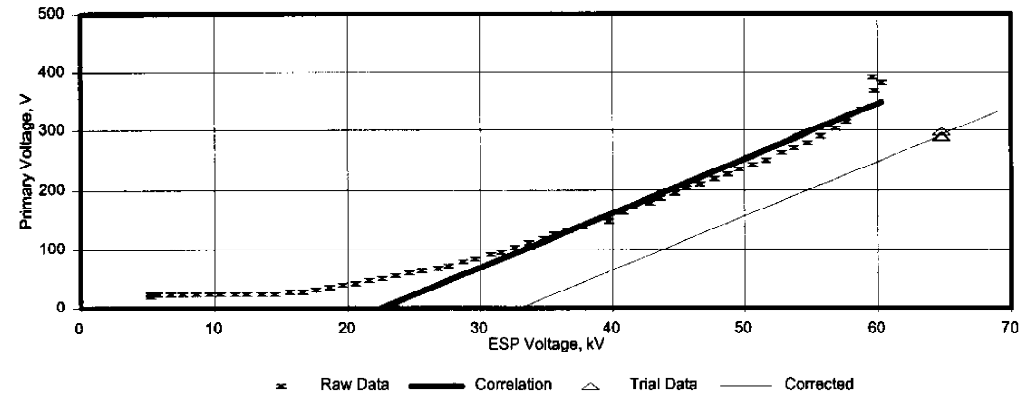
**TR Set 2-B1 Air Load Test ADJUSTED Correlation for ESPert
NYSEG's Milliken Station, March 1996**



ADJUSTED EQUATION: ESP Voltage (KV) = 18.5 x ESP Current (mA) ^ 0.236



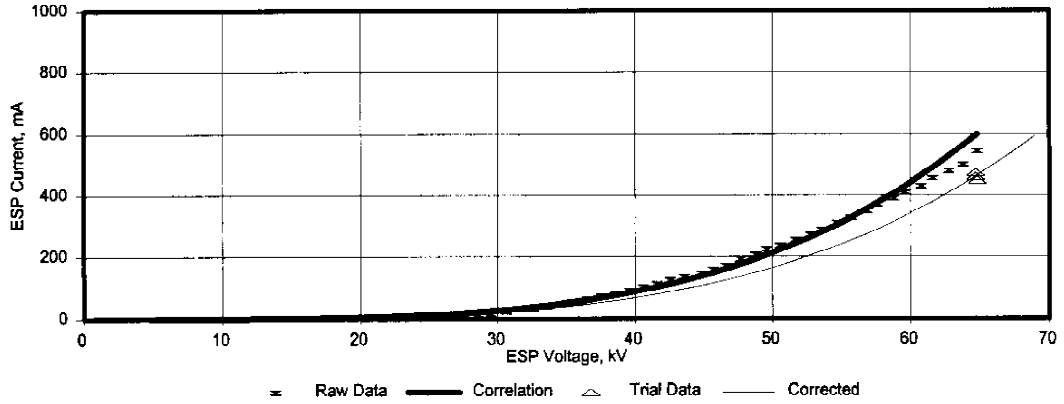
ADJUSTED EQUATION: Primary Current (A) = -0.58 + 0.182 x ESP Current (mA)



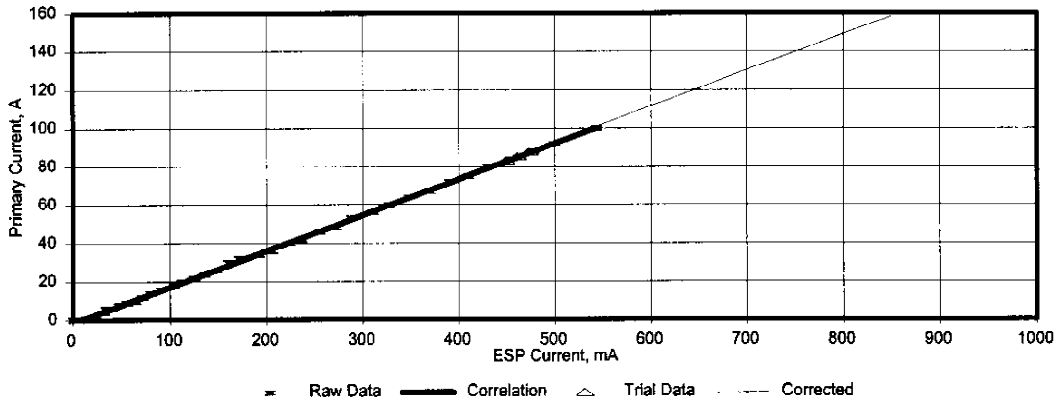
ADJUSTED EQUATION: Primary Voltage (V) = -303 + 9.20 x ESP Voltage (kV)

Figure 38

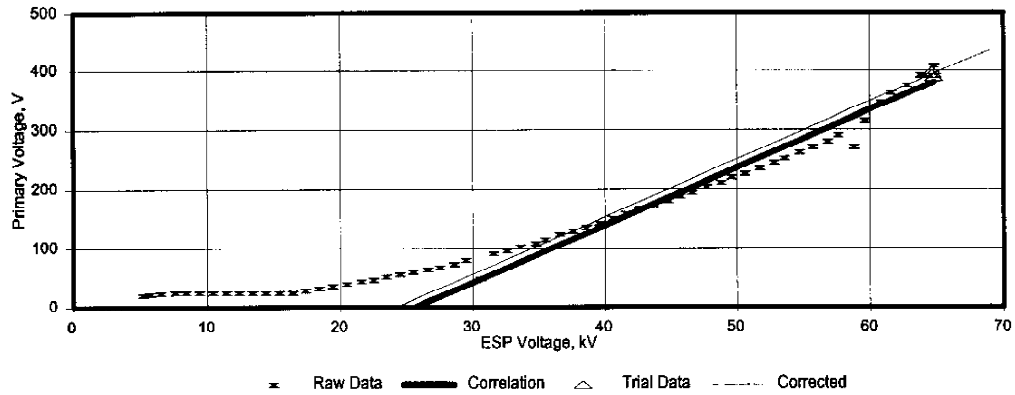
**TR Set 2-B2 Air Load Test ADJUSTED Correlation for ESPert
NYSEG's Milliken Station, March 1996**



ADJUSTED EQUATION: ESP Voltage (KV) = 14.0 x ESP Current (mA) ^ 0.250

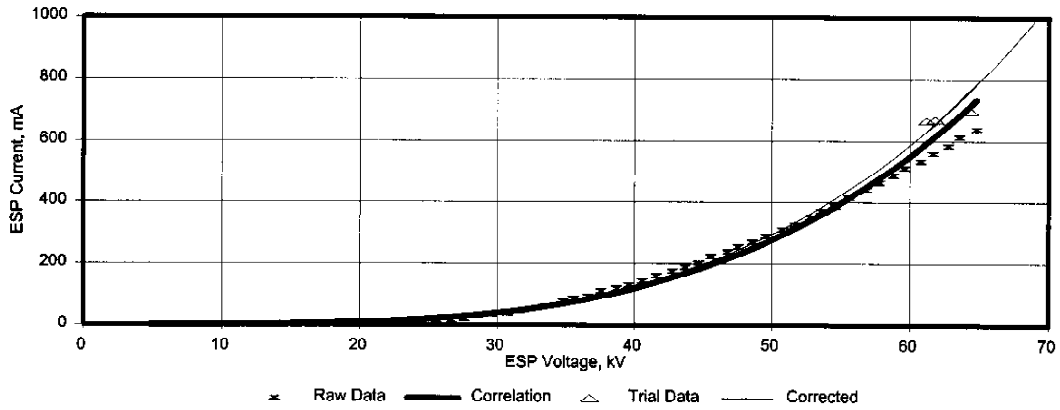


ADJUSTED EQUATION: Primary Current (A) = -0.81 + 0.187 x ESP Current (mA)

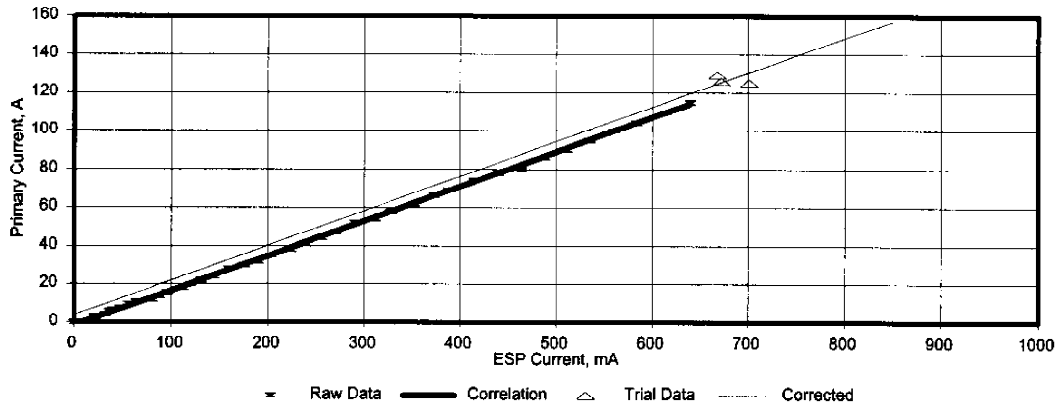


ADJUSTED EQUATION: Primary Voltage (V) = -236 + 9.72 x ESP Voltage (kV)

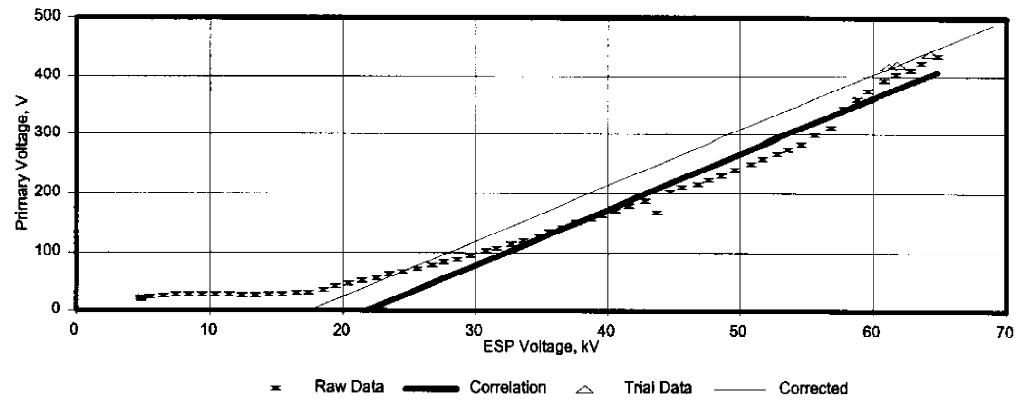
Figure 39
TR Set 2-B3 Air Load Test ADJUSTED Correlation for ESPert
NYSEG's Milliken Station, March 1996



ADJUSTED EQUATION: ESP Voltage (KV) = 11.0 x ESP Current (mA) ^ 0.266



ADJUSTED EQUATION: Primary Current (A) = 3.79 + 0.181 x ESP Current (mA)



ADJUSTED EQUATION: Primary Voltage (V) = -166 + 9.49 x ESP Voltage (kV)

Figure 40

Adjustments to ESPert Algorithms
 NYSEG's Milliken Station, Oct. 1995

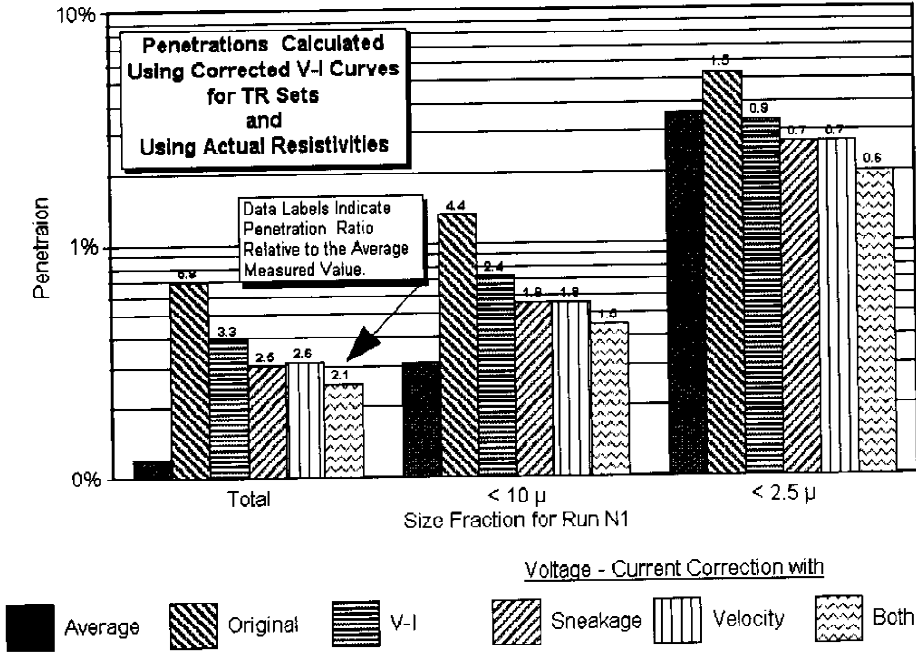


Figure 41

Adjustments to ESPert Algorithms
 NYSEG's Milliken Station, Oct. 1995

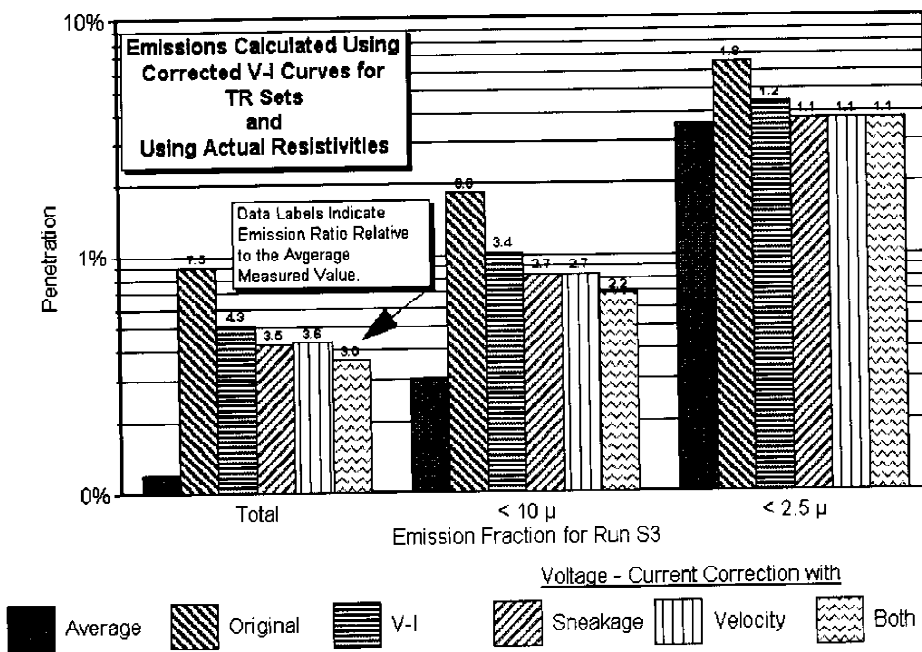


Figure 42

Rosin-Rammler Plot - Combined Inlet
NYSEG's Milliken Station, Oct. 1995

